

CELLULARITY FOR WEIGHTED KLRW ALGEBRAS OF TYPES B , $A^{(2)}$, $D^{(2)}$

ANDREW MATHAS AND DANIEL TUBBENHAUER

ABSTRACT. This paper constructs homogeneous affine sandwich cellular bases of weighted KLRW algebras in types $B_{\mathbb{Z}_{\geq 0}}$, $A_{2,e}^{(2)}$, $D_{e+1}^{(2)}$. Our construction immediately gives homogeneous sandwich cellular bases for the finite dimensional quotients of these algebras. Since weighted KLRW algebras generalize KLR algebras, we also obtain bases and cellularity results for the (infinite and finite dimensional) KLR algebras.

CONTENTS

| | |
|---|----|
| 1. Introduction | 1 |
| 2. Sandwich cellular algebras | 2 |
| 3. Reminders about weighted KLRW algebras | 4 |
| 4. The strategy | 9 |
| 5. The bases | 12 |
| 6. Proof of cellularity | 25 |
| 7. Table of notation and central concepts | 28 |
| References | 29 |

1. INTRODUCTION

KLR algebras, or quiver Hecke algebras, are graded infinite dimensional algebras attached to a quiver. These algebras arise in categorification and categorical representation theory, see e.g. [KL09], [KL11], [Rou08] or [Rou12]. They admit finite dimensional quotients, called *cyclotomic KLR algebras*. The KLR algebras and their cyclotomic quotients play crucial roles in modern representation theory and have attracted a lot of attention since their introduction.

A crucial problem is to determine whether these algebras are (graded) cellular in the sense of [GL96], or some variation of cellularity such as affine cellular [KX12]. It turns out that they tend to be graded affine cellular in the infinite dimensional case, see e.g. [KL15], and graded cellular in the finite dimensional case, see e.g. [HM10]. This paper gives explicit homogeneous (affine) cellular bases for these algebras. Moreover, we will see that there is a close relationship between the cellular bases of the infinite dimensional KLR algebras and their finite dimensional quotients, even though this is very hard to see directly in the KLR setting.

Weighted KLRW algebras are generalizations of KLR algebras that were introduced by Webster; see [Web19], [Web17], [Bow22] or [MT21]. Like the KLR algebras, the weighted KLRW algebras admit finite dimensional quotients. The KLR algebras can be constructed as idempotent subalgebras of the weighted KLRW algebras. Some care must be taken when comparing the weighted KLRW and KLR algebras because, for example, the functor induced by idempotent truncation annihilates some of the simple modules.

In the **AC types**, that is, types $A_{\mathbb{Z}}$, $A_e^{(1)}$, $C_{\mathbb{Z}_{\geq 0}}$, $C_e^{(1)}$, we showed [MT21] that one of the key properties of the weighted KLRW algebras is that they have homogeneous affine cellular bases constructed in the style of low dimensional topology, and these bases automatically descend to the finite dimensional quotients. As a result, we obtained homogeneous (affine) cellular bases for the corresponding KLR algebras and their finite dimensional quotients. Even better, all of these bases are defined over any commutative integral domain R (for example $R = \mathbb{Z}$).

It is natural to ask whether these constructions can be extended to other types. In this paper we answer this question affirmatively for types $B_{\mathbb{Z}_{\geq 0}}$, $A_{2,e}^{(2)}$, $D_{e+1}^{(2)}$: the **BAD types**. That is, we construct homogeneous affine sandwich cellular bases for weighted KLRW algebras that descend to the finite dimensional quotients. As in the **AC types**, we obtain bases for the corresponding KLR algebras. The sandwich part of our bases, corresponding to the finite dimensional quotients, is given by copies of the dual numbers $R[X]/(X^2)$, which explains the powers of 2 that appear in the dimension formulas of the finite dimensional KLR algebras. For completeness, we note that the weighted KLRW algebras and their finite dimensional quotients of **BAD types** are actually (affine) cellular; see Remark 2A.7 for a more precise statement. As a consequence,

Mathematics Subject Classification 2020. Primary: 16G99, 20C08; Secondary: 20C30, 20G43.

Keywords. KLR algebras, diagram algebras, cellular bases, Hecke and Schur algebras.

This picture has to be interpreted with care because, in general, we do not necessarily have such a factorization.

We use the following terminology for special cases:

- (a) A graded **affine sandwich cell datum** for A is a graded sandwich cell datum such that, for all $\lambda \in \mathcal{P}$ and for some $n(\lambda) \in \mathbb{Z}_{\geq 0}$, we have $\mathbb{S}_\lambda \cong R[X_1, \dots, X_{n(\lambda)}]$.
- (b) A graded **cell datum** for A is a graded sandwich cell datum such that $\mathbb{S}_\lambda \cong R$ for all $\lambda \in \mathcal{P}$.

The image of C in A is an **homogeneous sandwich cellular basis** for A . Similarly, we refer to affine sandwich cellular bases etc.

The following **Clifford–Munn–Ponizovskii theorem** parametrizes the simple modules of sandwich cellular algebras. To state this result we need some notions.

For each $\lambda \in \mathcal{P}$ there exists a cell module $\Delta(\lambda)$ and a cellular pairing ϕ^λ on $\Delta(\lambda)$, see [TV21, Section 2B]. The pairing ϕ^λ is a symmetric bilinear form. Let $\mathcal{P}^{\neq 0} \subset \mathcal{P}$ be the subset of those λ for which ϕ^λ is nonzero. The illustration to keep in mind is derived from [TV21, Section 2B], the details can be copied from [KX12, Section 2.2]:

$$\phi^\lambda \left(\begin{array}{c} a \\ \text{U} \\ b \end{array}, \begin{array}{c} b' \\ \text{D}' \end{array} \right) \rightsquigarrow \begin{array}{c} b' \\ \text{D}' \\ a \\ \text{U} \\ b \end{array} \leftarrow \phi^\lambda \left(\begin{array}{c} \text{U} \\ b \end{array}, \begin{array}{c} b' \\ \text{D}' \\ a \end{array} \right).$$

Theorem 2A.4. *Let R be a field, and let A be a graded sandwich cellular algebra.*

- (a) *All (graded) simple A -modules are uniquely associated to a $\lambda \in \mathcal{P}^{\neq 0}$, called their **apex**.*
- (b) *Assume that \mathbb{S}_λ is unital Artinian or commutative. For a fixed apex $\lambda \in \mathcal{P}^{\neq 0}$ there is a 1:1-correspondence*

$$\{\text{simple } A\text{-modules with apex } \lambda\} / \cong \xleftrightarrow{1:1} \{\text{simple } \mathbb{S}_\lambda\text{-modules}\} / \cong.$$

- (c) *Assume that \mathbb{S}_λ is unital graded Artinian or commutative. For a fixed apex $\lambda \in \mathcal{P}^{\neq 0}$ there is a 1:1-correspondence*

$$\{\text{graded simple } A\text{-modules with apex } \lambda\} / \cong \xleftrightarrow{1:1} \{\text{graded simple } \mathbb{S}_\lambda\text{-modules}\} / \cong.$$

Even for noncommutative \mathbb{S}_λ the assumption of being unital (graded) Artinian can be avoided under certain conditions, see [TV21, Section 2C] for details.

Proof. The proof is not very different from the general theory as in [GL96], [KX12], [AST18], [ET21], [GW15], [TV21] or [Tub22]. In particular, the result is just a (graded) reformulation of [GW15, Theorem 3] and [TV21, Section 2C]. Details are omitted. \square

Remark 2A.5. The bijection in [Theorem 2A.4](#) can be made explicit: the simple A -modules of apex $\lambda \in \mathcal{P}^{\neq 0}$ can be constructed as the simple heads of (adjustments of) the cell modules.

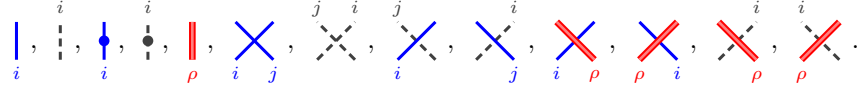
Remark 2A.6. The formulation of [Theorem 2A.4](#) is strongly inspired by Green's theory of cells (Green's relations) [Gre51], and the Clifford–Munn–Ponizovskii theorem of semigroup theory, see e.g. [GMS09] for a modern formulation.

Remark 2A.7. If A is involutive and all sandwiched algebras have an (affine sandwich) cellular datum compatible with the sandwich structure on A , then A also has a cell datum that can be constructed by refining the sandwich cell datum on A in an appropriate sense; see [TV21, Proposition 2.9]. However, refining the datum often makes the natural sandwich datum more cumbersome with very little gain. In our case, the sandwiched algebras are (copies of) polynomial rings and dual numbers, which are affine sandwich cellular algebras, so all of our algebras can be refined to an (affine sandwich) cell datum. Since these the representation theory of these algebras is well-understood, refining the sandwich cell datum for the weighted KLRW algebras in this paper appears to be unnecessary.

Notation 2A.8. From now on all of our algebras are assumed to be involutive, and we will omit the use of this word. We have separated the involutive condition (AC₅) in [Definition 2A.2](#) from the other axioms because being involutive is not necessary for [Theorem 2A.4](#) to hold.

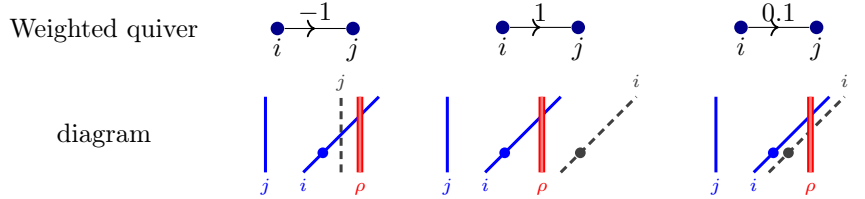
The n -tuple \mathbf{x} gives the x -coordinates of the n solid strings. For example, in (3A.2) above we have $\mathbf{x} = (1, 2, 3.25, 3.5, 4.5, 5.5, 7, 7.5)$. The ghost shift gives the distances between a solid string and its ghost, e.g. in (3A.2), the ghost shifts are 0.75 and 1.25 for the two edges starting a vertex 1 and 0.9 for other edge. Finally, $\boldsymbol{\kappa}$ gives the x -coordinates of the red strings and in (3A.2) we have $\boldsymbol{\kappa} = (0.75, 4)$. In general, the x -coordinates of the strings at the top and bottom of the diagrams will be different.

- (e) A set X of **positions**, which is the set of possible x -coordinates for the strings. We stress that the rank of the weighted KLRW algebra, which is the number of solid strings, strongly depends on the choice of X .
- (f) Diagrams consisting of n solid strings labeled by $i \in I$, their ghost strings (explained in the next bullet point), and ℓ red strings labeled by ρ . Solid and ghost strings can be decorated with dots. These diagrams are such that their internal points have local neighborhoods of the form



- (g) Let $\epsilon: i \rightsquigarrow j$ be an edge. If $\sigma_\epsilon > 0$ then each solid i -string has a ghost i -string that is shifted σ_ϵ units to the right. For each dot on the solid string there is a corresponding dot on the ghost string, which is shifted σ_ϵ units to the right. The ghost string is just a translate of the solid string, so it mimics its solid string. Similarly, if $\sigma_\epsilon < 0$ then each solid j -string has a ghost j -string that is shifted $-\sigma_\epsilon$ units to the right, together with any corresponding dots.

In (3A.2), each solid 0-string has one ghost shifted 0.9 units to the right. The solid 1-string has two ghosts, as there are two edges starting at 1, that are shifted 0.75 and 1.25 unit to the right. The solid 2-strings do not have any associated ghost strings, as no edges start from 2. Here are some more examples of these diagrams with a weighted quiver, where the edge weights gives the ghost shifts:



- (h) There is a degree function on these diagrams given by the local rules

$$\begin{aligned} \deg \begin{array}{c} \bullet \\ | \\ i \end{array} &= 2d_i, & \deg \begin{array}{c} \bullet \\ \bullet \\ | \\ i \end{array} &= 0, & \deg \begin{array}{c} \diagup \\ \diagdown \\ i \quad j \end{array} &= -\delta_{i,j} 2d_i, & \deg \begin{array}{c} \diagdown \\ \diagup \\ i \quad j \end{array} &= \deg \begin{array}{c} \diagup \\ \diagdown \\ i \quad j \end{array} = \begin{cases} \langle \alpha_i, \alpha_j \rangle & \text{if } i \rightsquigarrow j, \\ 0 & \text{else,} \end{cases} \\ \deg \begin{array}{c} \diagdown \\ \diagup \\ j \quad i \end{array} &= 0, & \deg \begin{array}{c} \diagdown \\ \diagup \\ i \quad j \end{array} &= \deg \begin{array}{c} \diagup \\ \diagdown \\ j \quad i \end{array} = \frac{1}{2} \delta_{i,j} \langle \alpha_i, \alpha_i \rangle, & \deg \begin{array}{c} \diagdown \\ \diagup \\ j \quad i \end{array} &= \deg \begin{array}{c} \diagup \\ \diagdown \\ i \quad j \end{array} = 0. \end{aligned}$$

Here, $\langle -, - \rangle$ is the Cartan pairing associated to Γ , and (d_0, \dots, d_e) is the symmetrizer.

The diagram in (3A.2) is of degree -1 with nonzero contributions given by -2 for the crossing with solid 0-strings, 1 twice for the solid 2-strings crossing the red 2-string, -2 for the crossing with solid 2-strings, and 1 for the crossing of a ghost 1 and a solid 2-string.

- (i) Let $\mathbf{u} = (u_1, \dots, u_n)$. If $f(\mathbf{u}) = u_1^{a_1} \dots u_n^{a_n} \in \mathbb{Z}_{\geq 0}[u_1, \dots, u_n]$ is a monomial, then $f(\mathbf{u})$ times a diagram is the same diagram but with a_k dots added at the top of the k th solid string, and all of its ghosts, for $1 \leq k \leq n$. Similarly, if $f(\mathbf{u}) \in \mathbb{Z}_{\geq 0}[u_1, \dots, u_n]$, then $f(\mathbf{u})$ times a diagram is the corresponding linear combination of diagrams.

Definition 3A.4. The **weighted KLRW algebra** $\mathscr{W}_n^\rho(X)$ is the graded unital associative R -algebra generated by such diagrams with multiplication given by stacking the diagrams and subject to the multilocal relations listed below. **Multilocal** relations need to be applied in local neighborhoods around the solid strings and, simultaneously, in the corresponding local neighborhoods around the ghost strings. See [Example 3A.8](#) below for an explicit example.

- (a) The **dot sliding relations** hold. That is, solid and ghost dots can pass through any crossing except:

$$(3A.5) \quad \begin{array}{c} \bullet \\ \diagdown \\ \diagup \\ i \quad i \end{array} - \begin{array}{c} \diagdown \\ \bullet \\ \diagup \\ i \quad i \end{array} = \begin{array}{c} | \\ | \\ i \quad i \end{array} = \begin{array}{c} \diagup \\ \bullet \\ \diagdown \\ i \quad i \end{array} - \begin{array}{c} \diagdown \\ \bullet \\ \diagup \\ i \quad i \end{array}.$$

Note that this relation may involve ghost strings, depending on whether edges in the quiver start from i . Here, and below, we omit strings for clarity unless they make a nontrivial contribution to the diagram.

(b) The *Reidemeister II relations* hold except in the following cases:

$$(3A.6) \quad \begin{array}{c} \text{Diagram 1: Crossing of two blue strings } i \text{ and } i. \\ \text{Diagram 2: Crossing of a blue string } i \text{ and a ghost string } j. \\ \text{Diagram 3: Crossing of a blue string } j \text{ and a ghost string } i. \end{array} = 0, \quad \begin{array}{c} \text{Diagram 4: Crossing of a blue string } i \text{ and a ghost string } j. \\ \text{Diagram 5: Crossing of a blue string } j \text{ and a ghost string } i. \end{array} = Q_{ij}(\mathbf{u}) \begin{array}{c} \text{Diagram 6: Blue string } i \text{ and ghost string } j. \\ \text{Diagram 7: Blue string } j \text{ and ghost string } i. \end{array} \text{ or } \begin{array}{c} \text{Diagram 8: Crossing of a blue string } i \text{ and a ghost string } j. \\ \text{Diagram 9: Crossing of a blue string } j \text{ and a ghost string } i. \end{array} = Q_{ji}(\mathbf{u}) \begin{array}{c} \text{Diagram 10: Blue string } i \text{ and ghost string } j. \\ \text{Diagram 11: Blue string } j \text{ and ghost string } i. \end{array} \text{ if } i \rightsquigarrow j, \\ \\ \begin{array}{c} \text{Diagram 12: Crossing of a red string } i \text{ and a blue string } i. \\ \text{Diagram 13: Crossing of a blue string } i \text{ and a red string } i. \end{array} = \begin{array}{c} \text{Diagram 14: Red string } i \text{ and blue string } i. \\ \text{Diagram 15: Blue string } i \text{ and red string } i. \end{array}.$$

(c) The *Reidemeister III relations* hold except in the following cases:

$$(3A.7) \quad \begin{array}{c} \text{Diagram 1: Crossing of a blue string } i \text{ and a ghost string } j. \\ \text{Diagram 2: Crossing of a blue string } j \text{ and a ghost string } i. \end{array} = \begin{array}{c} \text{Diagram 3: Crossing of a blue string } i \text{ and a ghost string } j. \\ \text{Diagram 4: Crossing of a blue string } j \text{ and a ghost string } i. \end{array} - Q_{iji}(\mathbf{u}) \begin{array}{c} \text{Diagram 5: Blue string } i \text{ and ghost string } j. \\ \text{Diagram 6: Blue string } j \text{ and ghost string } i. \end{array} \text{ or } \begin{array}{c} \text{Diagram 7: Crossing of a blue string } i \text{ and a ghost string } j. \\ \text{Diagram 8: Crossing of a blue string } j \text{ and a ghost string } i. \end{array} = \begin{array}{c} \text{Diagram 9: Crossing of a blue string } i \text{ and a ghost string } j. \\ \text{Diagram 10: Crossing of a blue string } j \text{ and a ghost string } i. \end{array} + Q_{ijji}(\mathbf{u}) \begin{array}{c} \text{Diagram 11: Blue string } i \text{ and ghost string } j. \\ \text{Diagram 12: Blue string } j \text{ and ghost string } i. \end{array} \text{ if } i \rightsquigarrow j, \\ \\ \begin{array}{c} \text{Diagram 13: Crossing of a red string } i \text{ and a blue string } i. \\ \text{Diagram 14: Crossing of a blue string } i \text{ and a red string } i. \end{array} = \begin{array}{c} \text{Diagram 15: Crossing of a red string } i \text{ and a blue string } i. \\ \text{Diagram 16: Crossing of a blue string } i \text{ and a red string } i. \end{array} - \begin{array}{c} \text{Diagram 17: Red string } i \text{ and blue string } i. \\ \text{Diagram 18: Blue string } i \text{ and red string } i. \end{array}.$$

The Reidemeister II or III relations without error terms are called *honest* Reidemeister relations.

The multilocal relations are sometimes tricky to apply but they are crucial for the combinatorics to work:

Example 3A.8. Consider the following two diagrams (in these pictures both solid i -strings have one ghost).

$$\begin{array}{c} \text{Diagram 1: Two solid } i \text{ strings.} \\ \text{Diagram 2: Two ghost } i \text{ strings.} \end{array} \stackrel{(3A.5)}{=} \begin{array}{c} \text{Diagram 3: Crossing of two solid } i \text{ strings.} \\ \text{Diagram 4: Crossing of a solid } i \text{ string and a ghost } i \text{ string.} \\ \text{Diagram 5: Crossing of a ghost } i \text{ string and a solid } i \text{ string.} \end{array}, \quad \begin{array}{c} \text{Diagram 6: Two solid } i \text{ strings.} \\ \text{Diagram 7: Two ghost } i \text{ strings.} \end{array} \text{ and } \begin{array}{c} \text{Diagram 8: Two solid } i \text{ strings.} \\ \text{Diagram 9: Two ghost } i \text{ strings.} \end{array}.$$

One cannot decide locally around just the two solid i -strings whether (3A.5) can be applied. In the left-hand diagram, the relation can be applied, giving the linear combination of diagrams above. In contrast, in the right-hand diagram relation (3A.5) cannot be applied because the two solid i -strings cannot be pulled arbitrarily close together using isotopies as the solid k -string prevents this from happening. \diamond

Remark 3A.9. Assume that a vertex $i \in I$ has multiple outgoing edges with positive weighting, so that there can be many ghost i -strings. For example:

$$\begin{array}{c} \text{Diagram 1: Quiver with vertices } 0, 1, 2. \\ \text{Diagram 2: Quiver with vertices } 1, 2. \end{array} \rightsquigarrow \begin{array}{c} \text{Diagram 3: Quiver with vertices } 1, 2. \\ \text{Diagram 4: Quiver with vertices } 1, 2. \end{array}.$$

Note that these two ghost strings are different strings that behave differently because the relations depend on the edges and on the residues. In the example above, the two ghost 1-strings play different roles. For example, one of them has nontrivial Reidemeister II relations with the 0-strings and the other has nontrivial Reidemeister II relations with the 2-strings.

Remark 3A.10. Note that [MT21] mostly works with $\mathscr{W}_\beta^\rho(X)$, where β determines the labels of the solid strings. This difference is not very important since $\mathscr{W}_n^\rho(X) = \bigoplus_{\beta \in Q_n^+} \mathscr{W}_\beta^\rho(X)$, where Q_n^+ is the set of positive roots of height n , which corresponds to the set of possible labels on the n solid strings.

A diagram is *unsteady* if it contains a solid string that can be pulled arbitrarily far to the right when the the red strings belong to region bounded by X , otherwise it is *steady*. For example, we have

$$(3A.11) \quad \text{Unsteady: } \begin{array}{c} \text{Diagram 1: Red string } \rho \text{ and blue string } i. \\ \text{Diagram 2: Red string } \rho \text{ and blue string } i. \end{array} \text{ pulls freely, } \quad \text{steady: } \begin{array}{c} \text{Diagram 3: Red string } i \text{ and blue string } \rho. \\ \text{Diagram 4: Red string } i \text{ and blue string } \rho. \end{array} \text{ stopped by the red string.}$$

Note that the ghost string mimics its parent solid string, so the solid i -string in the left diagram does indeed pull freely to the right.

Finally, the *cyclotomic weighted KLRW algebra* $\mathcal{R}_n^\rho(X)$ is the finite dimensional quotient of $\mathcal{W}_n^\rho(X)$ by the two-sided ideal generated by all diagrams that factor through an unsteady diagram.

3B. Duality and partners. We use the usual *diagrammatic antiinvolution* $(-)^*$ given by (the R -linear extension of) reflecting diagrams in their horizontal axis. This antiinvolution is the one we use for the homogeneous (affine) sandwich cellular basis. An illustration of the diagrammatic antiinvolution is:

$$\left(\begin{array}{c} j \quad i \\ \diagdown \quad \diagup \\ i \quad j \\ \rho \end{array} \quad \begin{array}{c} k \\ \diagdown \\ k \end{array} \right)^* = \begin{array}{c} i \quad j \\ \diagup \quad \diagdown \\ j \quad i \\ \rho \end{array} \quad \begin{array}{c} k \\ \diagup \\ k \end{array}.$$

There is a different kind of duality on diagrams, which exists because the relations (3A.5)–(3A.7) come in mirrored pairs. Explicitly, up to scalars, the set of relations is invariant under reflecting diagrams in their vertical axis and, in some circumstances, swapping solid strings with their ghosts. Most of the relations we will use have this type of duality, which we call *partner relations*. Note that the partner relations can have different scalars, however, this will not play a role for us because we only use partner relations when similar arguments can be applied to both relations.

For example, if $i \rightsquigarrow j$, then

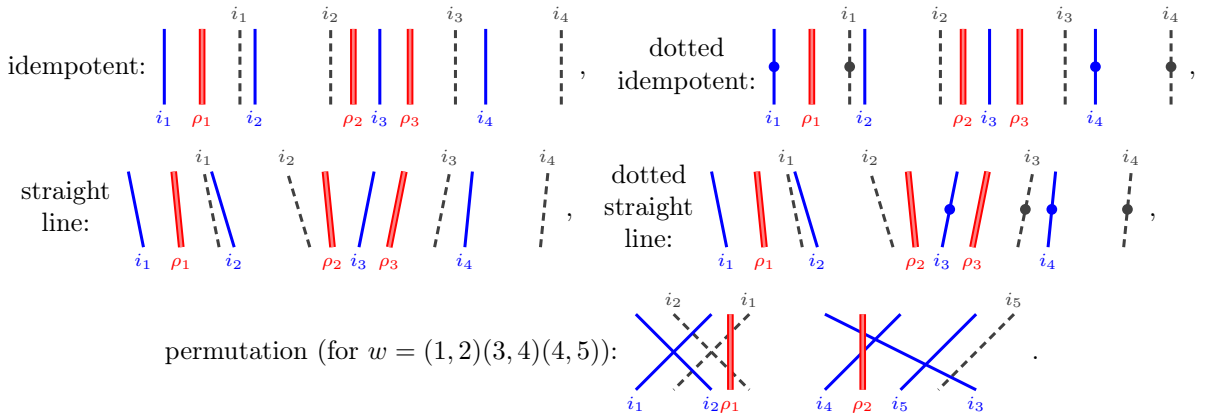
$$\begin{array}{c} i \quad i \\ \diagdown \quad \diagup \\ j \end{array} = \begin{array}{c} i \quad i \\ \diagup \quad \diagdown \\ j \end{array} - Q_{iji}(\mathbf{u}) \begin{array}{c} i \\ | \\ j \end{array} \begin{array}{c} i \\ | \\ j \end{array} \xleftrightarrow{\text{partner relations}} \begin{array}{c} i \\ \diagdown \quad \diagup \\ j \quad j \end{array} = \begin{array}{c} i \\ \diagup \quad \diagdown \\ j \quad j \end{array} + Q_{iji}(\mathbf{u}) \begin{array}{c} i \\ | \\ j \end{array} \begin{array}{c} i \\ | \\ j \end{array},$$

is an example of partner relations. Note the change of sign when going from left to right.

3C. Some diagrams that we need. We need certain special diagrams:

- (a) *Idempotent diagrams* are diagrams with no dots and no crossings, and fixed x -coordinates for all strings.
- (b) *Straight line diagrams* are diagrams with no dots and no crossings.
- (c) *Dotted idempotent diagrams* and *dotted straight line diagrams* are dotted diagrams of the respective type.
- (d) *Permutation diagrams* are diagrams with no dots such the solid strings correspond to a reduced expression of a permutation; see [MT21, Definition 3B.1] for a more precise definition.

Example 3C.1. Examples of these types of diagrams are:



These illustrate (dotted) idempotents, (dotted) straight line and permutation diagrams. \diamond

Notation 3C.2. Let $\mathbf{1}_{\mathbf{x}, \mathbf{i}}$ be the idempotent diagram with bottom boundary given by (\mathbf{x}, \mathbf{i}) , for $\mathbf{x} \in X$ and $\mathbf{i} \in I^n$. (That is, the positions and labels of the solid strings are given by \mathbf{x} and \mathbf{i} , respectively, when read from left to right.) As in Section 3A(i), given a polynomial $p(\mathbf{y}) \in R[y_1, \dots, y_n]$ write $p(\mathbf{y})\mathbf{1}_{\mathbf{x}, \mathbf{i}}$ for the corresponding linear combination of (dotted) diagrams $\mathbf{1}_{\mathbf{x}, \mathbf{i}}$.

Additionally, let $\mathfrak{S}_n = \langle s_1, \dots, s_{n-1} \rangle$ be the symmetric group on $\{1, \dots, n\}$ with $s_i = (i, i+1)$, which we think of as swapping the i th and $(i+1)$ th solid strings. For all $w \in \mathfrak{S}_n$ fix a reduced expression and let $D(w)$ be the associated permutation diagram. As often happens in the KLR world, the diagram $D(w)$ is only well-defined up to a choice of reduced expression and, as explained in [MT21, Definition 3B.1], some care needs to be taken. (These details are not important in this paper.)

4. THE STRATEGY

Our strategy to construct homogeneous (affine) sandwich cellular bases for the weighted KLRW algebras is the same as in [MT21, Remark 6.1], which we now recall. We will define the relevant notions later. The ideas are summarized in Remark 4A.1 and Example 4A.2 below.

Remark 4A.1. A crucial ingredient is the idea of using a certain form of *maximality*, with respect to string placement.

- (a) Fix a residue sequence $\mathbf{i}_\lambda = (i_1, \dots, i_n) \in I^n$. We construct an idempotent diagram $\mathbf{1}_\lambda$ by placing strings inductively as far to the right as possible. Here we use the fact that the relations in Definition 3A.4 only allow strings to be pulled to the right in certain situations, such as when they carry a dot. In this way, we think of previously placed strings as keeping the new string in check. One can think of this process as follows. We place the solid strings, and their ghosts, one at a time as follows. The positions of the red strings are determined by κ . Next, place the solid string of residue i_1 to the left of all of the red strings and pull it to the right using isotopies and the honest Reidemeister II relations until it is blocked by an (affine) red string. Now place the string of residue i_2 to the left of all of the strings and pull it to the right until it is blocked by an existing string. Repeat this process to place the remaining strings, starting at the left of the existing strings and pulling it to the right until it becomes stuck. The idempotent diagram $\mathbf{1}_\lambda$ is then a horizontal cut in the middle of the resulting diagram.

This ensures that $\mathbf{1}_\lambda$ is maximal with respect to placing the strings to the right. In fact, this strategy is a greedy algorithm, as it is designed to be locally maximal but it produces a globally maximal diagram.

- (b) By Definition 3A.4 again, when we put dots on the strings in $\mathbf{1}_\lambda$ it might be possible to pull some strings further to the right, so that the dotted idempotent diagram is no longer maximal with respect to string placement, and even more problematic, might become unsteady. In the finite dimensional case we consider only those dotted idempotent diagrams $y^f y_\lambda \mathbf{1}_\lambda$ that are steady. In the infinite dimensional case we even can add extra dots and get $y^a y^f y_\lambda \mathbf{1}_\lambda$. This gives a collection of dotted idempotent diagrams, which form the *middle* of the homogeneous (affine) sandwich cellular basis, in the sense of Remark 2A.3.
- (c) The (sandwich) cellular basis is then obtained by a standard construction for diagram algebras, which in our case means putting semistandard permutation diagrams above and below $y^a y^f y_\lambda \mathbf{1}_\lambda$.

The basis itself is maximal (in a certain sense), by construction, and it is not hard to prove that it is indeed a homogeneous (affine) sandwich cellular basis. For example, putting additional dots on the basis elements allows one pull strings and jump dots to the right, making the resulting diagram bigger. This gives an inductive way of proving results.

This strategy works perfectly in types $A_{\mathbb{Z}}$ and $A_e^{(1)}$, see [MT21], and requires small adjustments in the BAD types.

Example 4A.2. We now give an example of our main construction. This example is meant for the reader to come back as they read through the text, so not all of the notation is defined at this point. This example is in level 1 and there is one 0-red string.

- (a) Consider type $D_{2+1}^{(2)}$ and the following sequence of Young diagrams, adding nodes in row reading order, with the nodes filled with their residues.

$$\begin{array}{l}
 \emptyset \xrightarrow{0} (1) = \begin{array}{|c|} \hline 0 \\ \hline \end{array} \\
 \xrightarrow{1} (2) = \begin{array}{|c|c|} \hline 0 & 1 \\ \hline \end{array} \\
 \xrightarrow{2} (3) = \begin{array}{|c|c|c|} \hline 0 & 1 & 2 \\ \hline \end{array} \\
 \xrightarrow{2} (4) = \begin{array}{|c|c|c|c|} \hline 0 & 1 & 2 & 2 \\ \hline \end{array} \\
 \\
 \xrightarrow{0} (4, 1) = \begin{array}{|c|c|c|c|} \hline 0 & 1 & 2 & 2 \\ \hline & 0 & & \\ \hline \end{array} \\
 \xrightarrow{1} (4, 2) = \begin{array}{|c|c|c|c|} \hline 0 & 1 & 2 & 2 \\ \hline & 0 & 1 & \\ \hline \end{array} = \lambda.
 \end{array}$$

Write ψ_4 for the crossing of the solid 2-strings, which are the fourth and fifth strings read from the left. Then the basis set is

$$\{\mathbf{1}_\lambda^y, y_1 \mathbf{1}_\lambda^y, \psi_4 \mathbf{1}_\lambda^y, \psi_4 y_1 \mathbf{1}_\lambda^y, \mathbf{1}_\lambda^y \psi_4, y_1 \mathbf{1}_\lambda^y \psi_4, \psi_4 \mathbf{1}_\lambda^y \psi_4, \psi_4 y_1 \mathbf{1}_\lambda^y \psi_4\}.$$

For example, the diagram for $\psi_4 y_1 \mathbf{1}_\lambda^y \psi_4$ is

(4A.3) $\psi_4 y_1 \mathbf{1}_\lambda^y \psi_4 =$

The sandwiched algebra is the R -algebra spanned by $\mathbf{1}_\lambda^y$ and $y_1 \mathbf{1}_\lambda^y$, and this algebra is isomorphic to $R[X]/(X^2)$, with X in degree four, via $\mathbf{1}_\lambda^y \mapsto 1$ and $y_1 \mathbf{1}_\lambda^y \mapsto X$.

The graded dimension of the set of all cyclotomic weighted KLRW diagrams with $(0, 1, 2, 2, 0, 1)$ as their residue sequence at bottom and top is thus $q^2(1+q^{-2})^2(1+q^4)$, where we use q to keep track of the grading. \diamond

Notation 4A.4. Recall from Section 3A that we will draw *affine red strings* in diagrams, illustrated by:

$$\text{genuine red string : } \begin{array}{c} \color{red}{\parallel} \\ i \end{array}, \quad \text{affine red string : } \begin{array}{c} \color{green}{\parallel} \\ i \end{array}.$$

Importantly, the affine red strings are not part of the diagrams and they are drawn only as a visual aid.

The affine red strings are drawn to the right of all of the genuine red strings and we think of them as satisfying the same relations as the red strings. Our strategy is to pull strings as far to the right as possible but it is possible to pull some strings arbitrarily far to the right. The affine red strings are necessary to catch the solid strings that can be pulled past all of the genuine red strings in the diagram (we add enough affine red strings so as to be able to block all solid strings). By definition, a diagram is unsteady if and only if it contains a solid string that is blocked by an affine red string. As a vector space, the finite dimensional quotients of weighted KLRW algebras are spanned by those diagrams that do not have any strings blocked by affine red strings.

Example 4A.5. To show why the affine red strings are necessary consider a diagram with one red 0-string and one solid 1-string. For simplicity we do not draw the ghost strings. Using the honest Reidemeister II relation, the solid 1-string pulls arbitrarily far to the right:

In order to place the 1-string our strategy is to add an affine red 1-string to the right of the red string:

The solid 1-strings gets stuck at the affine red 1-string because it does not satisfy an honest Reidemeister II relation. (We add enough affine red strings to ensure that all strings are blocked.) \diamond

The following lemmas are the crucial diagrammatic relations that we need to pull strings and jump dots to the right. Here we are pulling the leftmost string to the right or jumping the leftmost dot to the right. We highlight the strings where the action happens by coloring them.

Lemma 4A.6. *For any quiver and any choice of Q -polynomials we have the following, plus partner relations:*

$$(4A.7) \quad \begin{array}{c} \color{green}| \color{blue}| \\ i \quad i \end{array} = \begin{array}{c} \color{blue} \bullet \\ \color{blue}| \color{blue}| \\ i \quad i \end{array} - \begin{array}{c} \color{blue} \bullet \\ \color{blue}| \color{blue}| \\ i \quad i \end{array}, \quad \begin{array}{c} \color{green}| \color{blue}| \\ i \quad i \end{array} = \begin{array}{c} \color{blue} \bullet \\ \color{blue}| \color{blue}| \\ i \quad i \end{array} + \begin{array}{c} \color{blue} \bullet \\ \color{blue}| \color{blue}| \\ i \quad i \end{array} - \begin{array}{c} \color{blue} \bullet \\ \color{blue}| \color{blue}| \\ i \quad i \end{array}.$$

For $i \rightarrow j$ edges and the choice of Q -polynomials in (3A.3) we have the following, plus partner relations:

$$(4A.8) \quad \begin{array}{c} \color{green} \bullet \\ \color{green}| \color{blue}| \\ i \quad j \end{array} = \begin{array}{c} \color{green} \bullet \\ \color{green}| \color{blue}| \\ i \quad j \end{array} + \begin{array}{c} \color{green} \bullet \\ \color{green}| \color{blue}| \\ i \quad j \end{array}, \quad \begin{array}{c} \color{green}| \color{blue}| \color{green}| \color{green}| \\ i \quad i \quad j \quad j \end{array} = - \begin{array}{c} \color{blue} \bullet \\ \color{blue}| \color{blue}| \\ i \quad i \end{array} \begin{array}{c} \color{green}| \color{green}| \\ i \quad i \end{array} - \begin{array}{c} \color{blue} \bullet \\ \color{blue}| \color{blue}| \\ i \quad i \end{array} \begin{array}{c} \color{green}| \color{green}| \\ i \quad i \end{array}.$$

The right relation and its partner also hold for $i \leftarrow j$.

For $i \Rightarrow j$ edges and the choice of Q -polynomials in (3A.3) we have the following, plus partner relations:

$$(4A.9) \quad \begin{array}{c} \color{green} \bullet \\ \color{green}| \color{blue}| \\ i \quad j \end{array} = \begin{array}{c} \color{green} \bullet \\ \color{green}| \color{blue}| \\ i \quad j \end{array} + \begin{array}{c} \color{green} \bullet \\ \color{green}| \color{blue}| \\ i \quad j \end{array}.$$

Proof. As in [MT21, Lemmas 6D.1, 6D.4 and 7E.1]. □

The relations (4A.8) and (4A.9) motivate the dot placement in Definition 5F.2 below: we construct our basis diagrams so that strings cannot be pulled, and dots cannot be jumped, further to the right, so we need to ensure that these relations cannot be applied.

Lemma 4A.10. *For $i \neq j$ and the choice of Q -polynomials in (3A.3) we have the following. In any close situation of the form*

$$\begin{array}{c} \color{green}| \color{blue}| \color{green}| \\ i \quad i \quad j \end{array},$$

we can pull the marked string further to the right. Similarly for its partner relations.

Proof. We first use (4A.7) to pull the left solid i -string into the middle. Note that this string also carries a dot after applying (4A.7). If $i \neq j$ are not connected, then either an honest Reidemeister II relation applies, or either (4A.8) or (4A.9) applies. In all cases, we can pull the leftmost solid i -string to the right. □

The next example should be compared with Remark 5D.10 below.

Example 4A.11. The following close configurations and their partners are stuck for $i \Rightarrow j$ and $i \leftarrow j$, respectively, so that Lemma 4A.6 and Lemma 4A.10 do not apply:

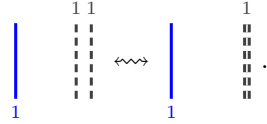
$$i \Rightarrow j: \begin{array}{c} \color{green}| \color{blue}| \color{green}| \\ i \quad i \quad j \end{array}, \quad i \leftarrow j: \begin{array}{c} \color{green}| \color{blue}| \color{green}| \\ i \quad i \quad j \end{array}.$$

These diagrams are therefore good in the sense that we can not pull strings or jump dots further to the right. These configurations will appear whenever i corresponds to a leaf of Γ . ◇

5. THE BASES

We now explain the main constructions of this paper. In Remark 6A.10 we summarize the parts of the arguments that are general and those that depend on the underlying quiver.

has ghost shift 1. As the 1-ghost strings are very close, we display them as doubled lines:



We stress that these are two different ghost 1-strings; cf. [Remark 3A.9](#). As in [Example 4A.2](#), when these strings have dots, we put a single ghost dot on the doubled ghost string rather than a dot on each ghost string.

We will draw generic diagrams that are supposed to make sense in any type, but the reader may need to remove or double some ghost strings to obtain the actual diagram for a particular type.

Definition 5B.6. Define the *affine charge* $\underline{\kappa} = (\underline{\kappa}_1, \dots, \underline{\kappa}_\ell) \in \mathbb{Z}^\ell$ and the *affine red labels* $\underline{\rho} = (\underline{\rho}_1, \dots, \underline{\rho}_\ell) \in I^\ell$ by

$$\underline{\kappa}_m = \begin{cases} \kappa_m & \text{if } 1 \leq m \leq \ell, \\ \kappa_\ell + 2n(m - \ell) & \text{otherwise,} \end{cases} \quad \text{and} \quad \underline{\rho}_m = \begin{cases} \rho_m & \text{if } 1 \leq m \leq \ell, \\ \lfloor \frac{m-\ell-1}{n} \rfloor + (e+1)\mathbb{Z} & \text{otherwise.} \end{cases}$$

We call $\underline{\kappa}_m$ and $\underline{\rho}_m$ the *position and residue* of a red string for $m \leq \ell$, and the *position and residue* of an affine red string for $m > \ell$.

Note that the coordinates of the (affine) red strings $\underline{\kappa}$ are always integers.

Example 5B.7. Take $n = 3$, $e = 2$ and $\ell = 1$, so $\underline{\ell} = 1 + 3 \cdot (2 + 1) = 10$. If $\kappa = (2)$ and $\rho = (1)$, then $\underline{\kappa} = (2, 8, 14, 20, 26, 32, 38, 44, 50, 56)$ and $\underline{\rho} = (1, 0, 0, 0, 1, 1, 1, 2, 2, 2)$. All entries, of $\underline{\kappa}$ and of $\underline{\rho}$, except the first are affine.

Below we will use this data to describe a diagram with red strings and affine red strings for the reason explained in [Example 4A.5](#). For example, the data above will give



In this example the positions of the strings are scaled to make it fit onto the page, the real positions are given by $\underline{\kappa} = (2, 8, 14, 20, 26, 32, 38, 44, 50, 56)$. Note that $n = 3$ and if we add n solid strings to this diagram from the left, and their ghosts, then we will see that each of these strings gets stuck somewhere. \diamond

5C. Partition combinatorics. Before coming to our main definitions, we introduce the tableau combinatorics that arise in *BAD* types. For the standard tableau combinatorics that appears in the context of KLR algebras we refer the reader to [\[HM10, Section 3.3\]](#).

Remark 5C.1. The partition combinatorics that we use is motivated by e.g. [\[AP14\]](#) and [\[AP16\]](#) who use the partitions of the crystal graphs for the affine fundamental weight. The associated weighted KLRW diagram combinatorics is a slight modification of the combinatorics of type $C_e^{(1)}$ as in [\[MT21, Section 7\]](#).

The reader should be careful because, as we will see, the partition combinatorics depends on ρ . In particular, the combinatorics from [\[AP14\]](#) and [\[AP16\]](#) only applies for cyclotomic KLR algebras for the fundamental weights associated to multisink vertices. This is related to the fact that the crystal graphs for fundamental weights indexed by multisink vertices have different indexing sets to the crystal graphs for the other fundamental weights.

Identify the vertices of I with $\mathbb{Z}/(e+1)\mathbb{Z}$. We use (*usual*) *partitions* of n , following the same conventions as in [\[MT21, Section 6A\]](#). We also use *shifted partitions* of n , that is, partitions λ with strictly decreasing parts $\lambda = (\lambda_1 > \dots > \lambda_k)$. (Shifted partitions are called *strict* partitions by some authors.) Let $|\lambda|$ be the size of a partition or shifted partition.

Definition 5C.2. The set of ρ -*partitions* is

$$\mathbb{P}_{\ell, n}^\rho = \left\{ (\lambda^{(1)} | \dots | \lambda^{(\ell)}) \left| \begin{array}{l} |\lambda^{(1)}| + \dots + |\lambda^{(\ell)}| = n, \text{ where} \\ \lambda^{(i)} \text{ is a usual partition if } \rho_i \text{ is not a multisink} \\ \lambda^{(i)} \text{ is a shifted partition if } \rho_i \text{ is a multisink} \end{array} \right. \right\}.$$

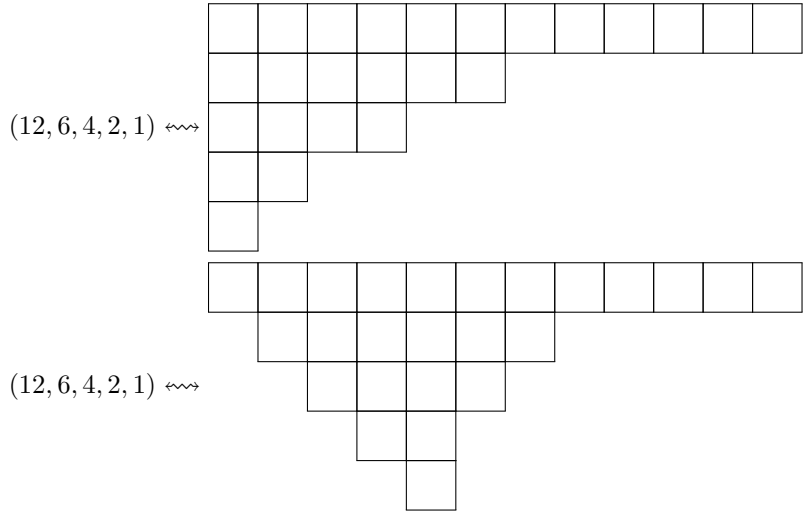
We define $\underline{\mathbb{P}}_{\ell, n}^\rho$ similarly using the indicated data.

We identify a ρ -partition λ with its *shifted ρ -Young diagram*, which is the set of nodes $\{(m, r, c)\}$ where $1 \leq m \leq \ell$, $\lambda_r^{(m)} > 0$, and

$$\begin{cases} 1 \leq c \leq \lambda_r^{(m)} & \text{if } \rho_m \text{ is not a multisink,} \\ 1 + r \leq c \leq \lambda_r^{(m)} + r & \text{if } \rho_m \text{ is a multisink.} \end{cases}$$

Remark 5C.3. In this paper a node (m, r, c) is in component m , row r and column c . This is different to the convention of e.g. [DJM98], where nodes are indexed in the order (r, c, m) . Our convention is better for this paper because in the representation theory the nodes are naturally ordered first by component and then by their row and column index, which is the lexicographic order on the nodes using our convention.

Notation 5C.4. We use the (shifted) English convention to illustrate the associated (*shifted*) ρ -Young diagrams. That is, we illustrate these partitions by drawing them as boxes in the plane, with rows ordered from top to bottom, and columns left to right, and where the r th row is shifted r positions to the right for shifted ρ -Young diagrams. (So the c th column of the r th row is in position $c + r$.) For example, a usual Young diagram and a shifted Young diagram are



This is a different convention to that used in [MT21, Sections 6 and 7] where the Russian convention is used. The Russian convention is useful in types $A_{\mathbb{Z}}$ and $A_e^{(1)}$, but seems to be irrelevant in other types.

That is, if ρ_i corresponds to a multisink vertex (i.e. the vertices e in all BAD types and, additionally, the vertex 0 in type $D_{e+1}^{(2)}$), then we consider shifted partitions in the i th entry of λ , and usual partitions otherwise. We make similar definitions as above for ρ -partitions. The nodes for $m > \ell$ are called *affine nodes*. Identify $P_{\ell, n}^{\rho}$ with the subset of $\underline{P}_{\ell, n}^{\rho}$ that consists of the $\underline{\rho}$ that do not contain any affine nodes.

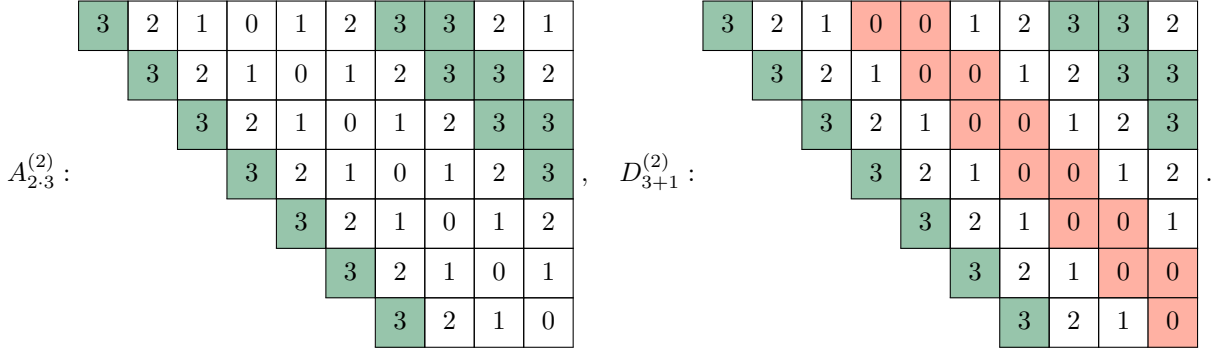
Definition 5C.5. Let $a = 1$ for type $A_{2, e}^{(2)}$ and $a = 2$ for type $D_{e+1}^{(2)}$. Given an integer $k \in \mathbb{Z}$ we need the remainder of division by $2e + a$ (viewed as an element of $\{0, \dots, 2e + a\} \subset \mathbb{Z}_{\geq 0}$), which we denote by $\text{Mod}(k, 2e + a)$. Define the *residue function* $r: \mathbb{Z} \rightarrow I$ by

$$r(k) = \begin{cases} \text{Mod}(k, 2e + a) + (e + 1)\mathbb{Z} & \text{if } 0 \leq \text{Mod}(k, 2e + a) \leq e, \\ 2e + 1 - \text{Mod}(k, 2e + a) + (e + 1)\mathbb{Z} & \text{if } e < \text{Mod}(k, 2e + a) < 2e + a. \end{cases}$$

The (ρ -)residue of the node (m, r, c) is $\text{res}_{\rho}(m, r, c) = r(c - r) + \rho_m + (e + 1)\mathbb{Z}$.

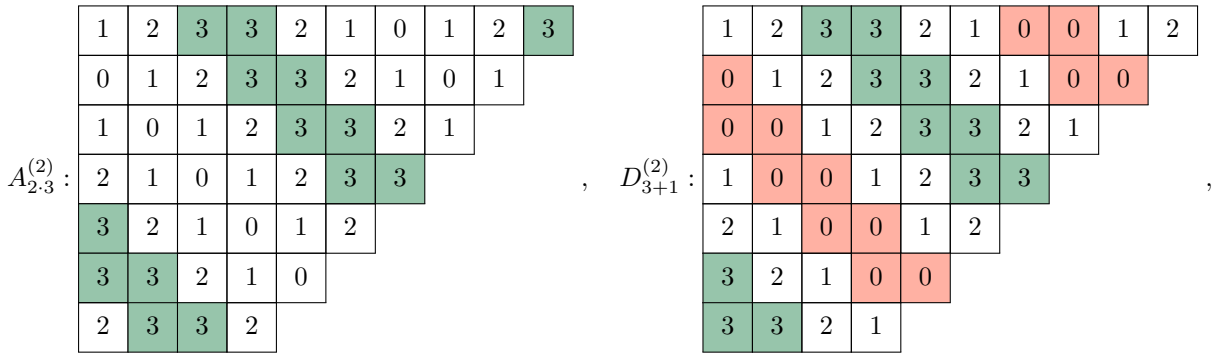
In illustrations we will often fill nodes with their residues. As the next example shows, the formal definition is more complicated than the actual concept of a residue.

Example 5C.6. For $\lambda = (10, 9, 8, 7, 6, 5, 4)$ and $e = 3$, starting with 3, i.e. $\rho = (3)$, we get:



Note that colored/shaded residues, for multisinks, are doubled. In words, the residues increase along rows and columns until they hit e , this value is doubled, and then the residues bounce back until they hit 0, this value is doubled for $D_{e+1}^{(2)}$, and the process starts again.

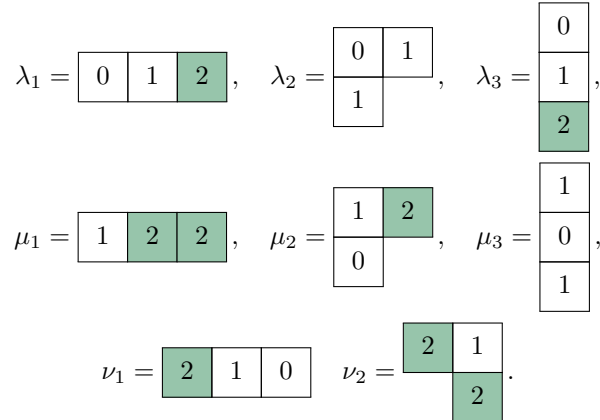
In contrast, if $\rho = (1)$, then



following Definition 5C.2. For $\rho = (2)$ the situation is similar. For $\rho = (0)$ type $A_{2,3}^{(2)}$ has partition, and type $D_{3+1}^{(2)}$ has shifted partition, combinatorics. We emphasize that, in general, there are more partitions than shifted partitions, so there are more of these diagrams when ρ_i is not a multisink. \diamond

The coloring/shading from Example 5C.6 distinguishes between usual and shifted partition combinatorics: we use shifted partition combinatorics if and only if the first node is colored/shaded.

Example 5C.7. We continue with Example 5B.7 and fix type $A_{2,2}^{(2)}$. There are three usual and two shifted 1-partitions of 3 and eight in total, namely (filled with their residues):



We get $P_{\ell,n}^\rho = \{\lambda_1, \lambda_2, \lambda_3\}$, if $\rho = (0)$, $P_{\ell,n}^\rho = \{\mu_1, \mu_2, \mu_3\}$, if $\rho = (1)$, and $P_{\ell,n}^\rho = \{\nu_1, \nu_2\}$, for $\rho = (2)$.

The set $\underline{P}_{\ell,n}^{\rho,all}$ is much bigger, and we will not list it here. Note, however, that the affine components of $\underline{P}_{\ell,n}^{\rho,all}$ have either usual or shifted partition combinatorics depending in the residue. More precisely, since $\underline{\rho} = (\rho, 0, 0, 0, 1, 1, 1, 2, 2, 2)$ we get that the first six affine components of $\underline{P}_{\ell,n}^{\rho,all}$ use usual partitions and the last three components use shifted partition combinatorics. \diamond

Remark 5C.8. In examples, and in the proofs below, we will mostly focus on the shifted partition combinatorics. The arguments for the usual partition combinatorics requires only slight adjustments and is essentially identical to that used for type $C_e^{(1)}$ in [MT21, Section 7].

5D. The idempotents. We now introduce some crucial definitions for defining the idempotent diagrams. For any $r + (e + 1)\mathbb{Z} \in I$, with $r \in \{0, \dots, e\}$, we sometimes abuse notation and identify $r + (e + 1)\mathbb{Z}$ with the real number in $r \in \mathbb{R}$. The meaning of the following definition is clarified in [Remark 5D.5](#) below.

Definition 5D.1. Define the **content function** (for the m th component) $c^m : I \rightarrow \mathbb{R}$ by

$$c^m(r) = \begin{cases} 2 - \rho_m & \text{if } \rho_m \neq 0, r = 0 \text{ and we are in type } D_{e+1}^{(2)}, \\ r - 2 & \text{if } \rho_m = 0, r \neq 0 \text{ and we are in type } D_{e+1}^{(2)}, \\ r - \rho_m & \text{otherwise.} \end{cases}$$

Recall the shift ε from [Notation 5B.2](#). Below we define the **positioning function**, which uses the **row reading order** $o_\lambda(m, r, c) = c + \sum_{i=1}^{r-1} \lambda_i^{(m)}$, which is the lexicographic order on the nodes.

Example 5D.2. The function $o_\lambda(-)$ returns the position of a node in a Young diagram when reading along rows, i.e. reading first left to right, and then bottom to top. So $o_\lambda(m, r, c) = k$ if (m, r, c) is the k th node in row reading order. This is be illustrated by

$$\left(\begin{array}{|c|c|c|} \hline 1 & 2 & 3 \\ \hline \end{array}, \begin{array}{|c|c|} \hline 4 & 5 \\ \hline 6 & \\ \hline \end{array}, \begin{array}{|c|} \hline 7 \\ \hline 8 \\ \hline 9 \\ \hline \end{array} \right),$$

where we filled the nodes with their value $o_\lambda(m, r, c)$. ◇

Notation 5D.3. From now on we always order nodes, and strings associated to nodes, by the row reading order.

Definition 5D.4. Let $\lambda \in \underline{\mathbb{P}}_{\ell, n}^{\rho, all}$. The **coordinate** of the node $(m, r, c) \in \lambda$ is

$$\mathbf{x}_\kappa(m, r, c) = \underline{\kappa}_m - \frac{m}{\ell} + c^m(r(k)) - k\varepsilon, \quad \text{where } k = o_\lambda(m, r, c).$$

The **coordinates** $\mathbf{x}_\kappa(\lambda)$ of λ is the ordered tuple of the coordinates of its nodes listed in row reading order.

The real number $\mathbf{x}_\kappa(m, r, c)$ will be the x -coordinate of the corresponding string in the idempotent diagram $\mathbf{1}_\lambda$. Moreover, [Definition 5D.4](#) looks more complicated than it actually is. The coordinate function simply places strings in order, following the strategy outlined in [Remark 4A.1](#).

Remark 5D.5. The contributions of the different ingredients of $\mathbf{x}_\kappa(m, r, c)$ are the following:

- (a) The x -coordinates of the nodes in the component $\lambda^{(m)}$ are centered around $\underline{\kappa}_m$, the position of the m th (affine) red string.
- (b) The $\frac{m}{\ell}$ differentiates between the components in the sense that the multiple of $\frac{1}{\ell}$ uniquely identifies the component of the node.
- (c) $c^m(r(k))$ ensures that strings with the same residue are placed within a certain region. The first two cases in the definition of c^m takes care of the 0 multisinks, which have special combinatorics, and the shift by ρ_m ensures that coordinates of residue ρ_m are the rightmost coordinates.
- (d) $-k\varepsilon$ ensures that nodes move a little bit to the left as we read along rows.

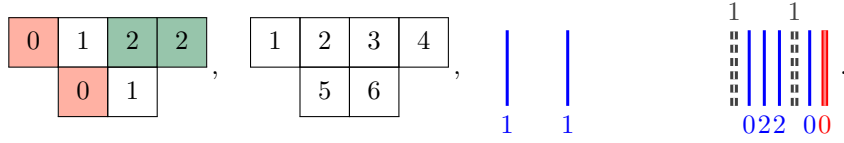
Note that in type $D_{e+1}^{(2)}$ the solid 0-strings and the solid 2-strings have roughly the same coordinates. This is important because the solid 0-strings do not have ghosts, but the solid 1-strings have two ghosts.

Example 5D.6. We continue with [Example 5C.7](#). Fix from now on $\kappa = (0)$. We have the following coordinates of ν_1 and ν_2 :

$$\begin{aligned} \mathbf{x}_\kappa(\nu_1) &= (-\varepsilon, -1 - 2\varepsilon, -2 - 3\varepsilon), & \begin{array}{|c|c|c|} \hline -\varepsilon & -1-2\varepsilon & -2-3\varepsilon \\ \hline \end{array} & \xrightarrow{\varepsilon \rightarrow 0} & \begin{array}{|c|c|c|} \hline 0 & -1 & -2 \\ \hline \end{array}, \\ \mathbf{x}_\kappa(\nu_2) &= (-\varepsilon, -1 - 2\varepsilon, -3\varepsilon), & \begin{array}{|c|c|} \hline -\varepsilon & -1-2\varepsilon \\ \hline & -3\varepsilon \\ \hline \end{array} & \xrightarrow{\varepsilon \rightarrow 0} & \begin{array}{|c|c|} \hline 0 & -1 \\ \hline & 0 \\ \hline \end{array}. \end{aligned}$$

We have illustrated the coordinates for the nodes in the shifted Young diagrams, and also what happens in the limit $\varepsilon \rightarrow 0$. Note that we have omitted the additional shift of $\frac{m}{\ell} = \frac{1}{10}$. ◇

Example 5D.7. Let us continue with [Example 4A.2](#), where $n = 6$ and $e = 2$. As before, $\lambda = (4, 2)$. We label the nodes of λ in row reading order and reproduce the associated idempotent diagram:



Let us assume that the red 0-string is placed at 0 and this is the only component, i.e. $\kappa = (0)$, $\ell = 1$ and $m = 1$. We then have $\underline{\ell} = 1 + 6 \cdot (2 + 1) = 19$ and $\frac{m}{\underline{\ell}} = \frac{1}{19} \approx 0.053$. Let us fix $\varepsilon = 0.001$. The solid strings displayed in [Example 4A.2.\(a\)](#) are at positions

$$\mathbf{x}_{\underline{\kappa}}(\lambda) \approx (-0.054, -1.055, -0.056, -0.057, -0.058, -1.059) \xrightarrow[\text{left to right}]{\text{ordered}} (-1.059, -1.055, -0.058, -0.057, -0.056, -0.054).$$

Here, $\mathbf{x}_{\underline{\kappa}}(\lambda)$ lists the positions in row reading order while, on the right-hand side, we list the coordinates for the solid strings with increasing x -coordinates from left to right. Note that the illustrated idempotent diagram is scaled to avoid clutter: the distance between the two solid 1-string is ≈ 0.01 while the distance from the solid 1-strings to the red 0-string is ≈ 1 .

Finally, filling the nodes of λ with their positions in \mathbb{R} gives:



In this sense one can think of $\mathbf{x}_{\underline{\kappa}}(\lambda)$ as a reading function on Young diagrams that associates a real number to each node in a controlled way, which corresponds to the strategy outlined in [Remark 4A.1](#). \diamond

We write $\max_{\mathbb{R}}(\text{fin})$, the *maximal finite part*, for the maximum of $\mathbf{x}_{\underline{\kappa}}$ on $\mathbb{P}_{\underline{\ell}, n}^{\rho}$, and call coordinates with $\mathbf{x}_{\underline{\kappa}}(m, r, c) > \max_{\mathbb{R}}(\text{fin})$ *affine*.

Lemma 5D.8. *The nodes with affine coordinates are precisely the affine nodes.*

Proof. Easy and omitted. \square

We now define the *idempotent diagrams* $\mathbf{1}_{\lambda}$ associated to $\lambda \in \mathbb{P}_{\underline{\ell}, n}^{\rho, \text{all}}$. Dotted idempotents will appear in [Section 5E](#).

Definition 5D.9. For $\lambda \in \mathbb{P}_{\underline{\ell}, n}^{\rho, \text{all}}$ let $\mathbf{1}_{\lambda}$ be the idempotent diagram given by:

- (a) placing ℓ red strings with labels given by ρ at coordinates given by κ , and,
- (b) n solid strings with labels $\text{res}_{\rho}(m, r, c)$ at coordinates $\mathbf{x}_{\underline{\kappa}}(m, r, c)$, for $(m, r, c) \in \lambda$.

The reader is now invited to go back to [Example 4A.2](#) and compare the idempotent diagrams appearing there with [Definition 5D.9](#). See [Example 5E.6](#) below for more examples.

As mentioned already, in diagrams we often draw affine red strings at positions κ_m , for $\ell < m \leq \underline{\ell}$, even though these strings are not strictly part of the diagram.

Remark 5D.10. In AC types the crucial illustrations that we used to show that our bases span the weighted KLRW algebras are [[MT21](#), (6A.10), (6A.11), (7A.8), (7A.9) and (7A.10)]. These diagrams identify local configurations of nodes in Young diagrams with local configurations of strings in diagrams. The analogs of these results the current setting, together with the Young diagram and the residues of the nodes, are as follows.

Assuming that the middle node is not 0 or e , and we do not have $i - 2 = 0$, $i = 0$ or $i + 2 = 0$ in type $D_{e+1}^{(2)}$, we have:

$$(5D.11) \quad \begin{array}{|c|c|c|} \hline i & i+1 & i+2 \\ \hline \end{array} \longleftrightarrow \begin{array}{c} | \\ \vdots \\ i \\ | \\ i+1 \\ | \\ i+2 \\ | \\ \vdots \end{array}, \quad \begin{array}{|c|c|c|} \hline i & i-1 & i-2 \\ \hline \end{array} \longleftrightarrow \begin{array}{c} | \\ \vdots \\ i-2 \\ | \\ i-1 \\ | \\ i \\ | \\ \vdots \end{array}.$$

The special cases in [Definition 5D.1](#) for type $D_{e+1}^{(2)}$ correspond to the local string configurations:

$$(5D.12) \quad \begin{array}{|c|c|c|} \hline 0 & 1 & 2 \\ \hline \end{array} \longleftrightarrow \begin{array}{c} | \\ \vdots \\ 1 \\ | \\ 2 \\ | \\ \vdots \end{array}, \quad \begin{array}{|c|c|c|} \hline 2 & 1 & 0 \\ \hline \end{array} \longleftrightarrow \begin{array}{c} | \\ \vdots \\ 1 \\ | \\ 0 \\ | \\ \vdots \end{array}.$$

That the two cases in (5D.11) and (5D.12) look different is an artifact of our conventions for ghost strings. However, this can not be avoided (meaning that one always gets special behavior) in type $D_{e+1}^{(2)}$ as there is no way to orient the quiver from left to right, or right to left.

When the middle residue is 0 or e we have:

$$(5D.13) \quad \begin{aligned} A_{2,e}^{(2)} : & \begin{array}{|c|c|c|} \hline 1 & 0 & 1 \\ \hline \end{array} \rightsquigarrow \begin{array}{c} | \\ 0 \end{array} \begin{array}{c} 0 \\ | \\ | \\ | \\ 11 \end{array} \begin{array}{c} 11 \\ | \\ | \\ | \\ \end{array}, \quad D_{e+1}^{(2)} : \begin{array}{|c|c|c|c|} \hline 1 & 0 & 0 & 1 \\ \hline \end{array} \rightsquigarrow \begin{array}{c} | \\ 1 \end{array} \begin{array}{c} | \\ 1 \end{array} \begin{array}{c} 1 \\ | \\ | \\ | \\ | \\ | \\ 00 \end{array}, \\ A_{2,e}, D_{e+1}^{(2)} : & \begin{array}{|c|c|c|c|} \hline e-1 & e & e & e-1 \\ \hline \end{array} \rightsquigarrow \begin{array}{c} | \\ e-1 \end{array} \begin{array}{c} | \\ e-1 \end{array} \begin{array}{c} e-1 \\ | \\ | \\ e \end{array} \begin{array}{c} e-1 \\ | \\ | \\ e \end{array}. \end{aligned}$$

These should be compared to Example 4A.11. Note that in all cases we cannot pull the strings for the middle node further to the right using the Reidemeister II relations, which is the point of these diagrams.

Whenever we have a multisink Remark 4A.1.(b) fails because flanking two solid i -strings with two crossings annihilates a diagram by (3A.6). This is not desirable because we want these diagrams to form the middle of a sandwich cellular basis. In Definition 5E.1 below, we will place a dot on such strands to avoid this problem. The picture to keep in mind is:

$$\text{no dots } \begin{array}{c} \diagup \\ \diagdown \\ \diagdown \\ \diagup \\ i \quad i \end{array} = 0 \quad \text{but} \quad \text{with a dot } \begin{array}{c} \diagup \\ \diagdown \\ \cdot \\ \diagdown \\ \diagup \\ i \quad i \end{array} \neq 0.$$

Finally, assuming that $|i - j| \leq 1$ in these pictures:

$$(5D.14) \quad \begin{array}{|c|c|c|c|} \hline k \mp 1 & \dots & j & i \\ \hline k & & & \\ \hline \end{array} \quad \text{or} \quad \begin{array}{|c|c|c|c|} \hline k & \dots & j & i \\ \hline & k & & \\ \hline \end{array} \rightsquigarrow \left\{ \begin{array}{l} \begin{array}{c} | \\ | \\ | \\ i \quad i \quad i \end{array} \begin{array}{c} i \quad i \quad i \\ | \\ | \\ | \\ \end{array} \\ \begin{array}{c} | \\ | \\ i \quad i \end{array} \begin{array}{c} i \quad i \\ | \\ | \\ \end{array} \\ \begin{array}{c} | \\ i \end{array} \begin{array}{c} i \\ | \\ k \end{array} \begin{array}{c} k \\ | \\ \end{array} \quad \text{or} \quad \begin{array}{c} | \\ k \end{array} \begin{array}{c} k \\ | \\ i \end{array} \begin{array}{c} i \\ | \\ \end{array} \end{array} \right. \begin{array}{l} \text{if } i = k = j \\ \text{is a multisink,} \\ \\ \text{if } i = k \neq j, \\ \\ \text{if } |k - i| = 1, \\ \\ \text{otherwise,} \\ \text{the solid/ghost } k\text{-string is close} \\ \text{to a ghost/solid } (k \pm 1)\text{-string} \end{array}$$

where the j -string is only illustrated in the top diagram, and in the last case the i and k -strings do not need to be close (neither the solids nor the ghosts). Note that in the shifted Young diagram $k = \rho_k$.

5E. The dotted idempotents. We now explain how we place dots on the idempotent diagram $\mathbf{1}_\lambda$.

Definition 5E.1. Suppose $\lambda \in \underline{P}_{\ell,n}^{\rho,all}$ and suppose that $(m, r, c), (m, r', c') \in \lambda$ with $k = o_\lambda(m, r, c)$ and $k + 1 = o_\lambda(m, r', c')$. If ρ_m is not a multisink (so usual partitions), then

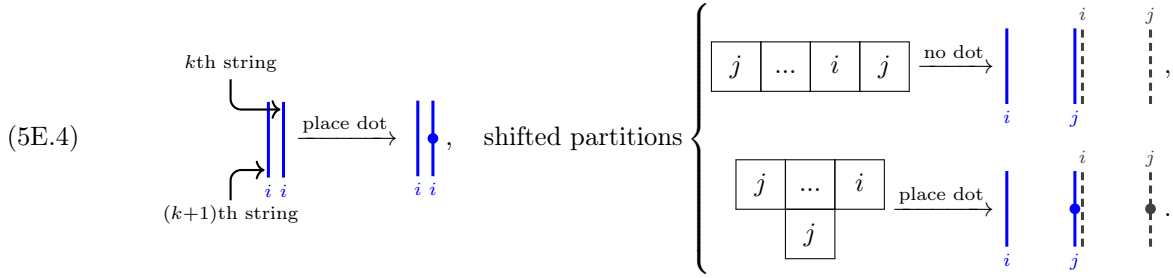
$$(5E.2) \quad a_k = \begin{cases} 1 & \text{if } \text{res}_\rho(m, r, c) = \text{res}_\rho(m, r + 1, 1), \\ 0 & \text{otherwise.} \end{cases}$$

If ρ_m is a multisink (so shifted partitions), then

$$(5E.3) \quad a_k = \begin{cases} 1 & \text{if } \text{res}_\rho(m, r, c) = \text{res}_\rho(m, r', c'), \text{ or } r' > 1 \text{ and } c' = 1, \\ 0 & \text{otherwise.} \end{cases}$$

The *dotted idempotent* associated to λ is $\mathbf{1}_\lambda^y = y_\lambda \mathbf{1}_\lambda$, where $y_\lambda = y_1^{a_1} \dots y_n^{a_n} \in R[y_1, \dots, y_n]$.

In other words, (5E.3) places a dot whenever the k th and the $(k+1)$ th string are close and have the same residue, and takes care of new rows as in (5D.14), e.g.:



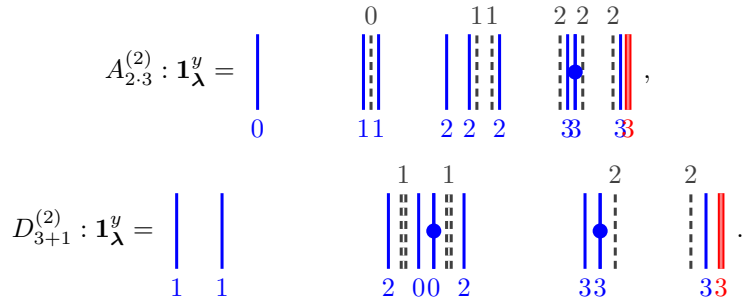
In the case of usual partitions the dot placement is the same as in type $C_e^{(1)}$ from [MT21, Section 7], see also (5E.9) below. Note that $\mathbf{1}_\lambda^y$ has zero or one dot on each strand. For example, the top diagram in (5D.14) gets two dots, one on the middle and one on the rightmost string.

Remark 5E.5. The dot placement in Definition 5E.1 is local to the components of the (shifted) partitions. This appears to be different to what is done in the KLR world where dots corresponding to later components are added to idempotents; see, for example, [HM10, Definition 4.9]. In fact, the red strings implicitly add dots to the idempotent diagrams via (3A.6), so these two pictures are compatible but different in flavor. Note since weighted KLRW algebras generalize KLR algebras the above dot placement gives a new way to think about cellular bases constructions in the KLR world.

Example 5E.6. We list a few examples of the dotted idempotents $\mathbf{1}_\lambda^y$ for $\ell = 1$ and $\kappa = (0)$.

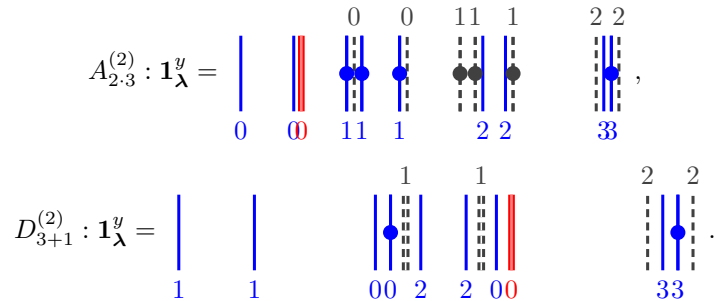
(a) Consider $\lambda = (9)$ for $e = 3$ and $\rho = (3)$. We get:

$$A_{2,3}^{(2)} : \begin{array}{|c|c|c|c|c|c|c|c|c|} \hline 3 & 2 & 1 & 0 & 1 & 2 & 3 & 3 & 2 \\ \hline \end{array}, \quad D_{3+1}^{(2)} : \begin{array}{|c|c|c|c|c|c|c|c|c|} \hline 3 & 2 & 1 & 0 & 0 & 1 & 2 & 3 & 3 \\ \hline \end{array}.$$



In contrast, if we instead have $\rho = (0)$, then we get

$$A_{2,3}^{(2)} : \begin{array}{|c|c|c|c|c|c|c|c|c|} \hline 0 & 1 & 2 & 3 & 3 & 2 & 1 & 0 & 1 \\ \hline \end{array}, \quad D_{3+1}^{(2)} : \begin{array}{|c|c|c|c|c|c|c|c|c|} \hline 0 & 1 & 2 & 3 & 3 & 2 & 1 & 0 & 0 \\ \hline \end{array}.$$



Note the different dot placement: for type $A_{2,3}^{(2)}$ we use (5E.2), while for $D_{3+1}^{(2)}$ we use (5E.3).

(b) Next, we illustrate the dotted idempotents for $\lambda = (8, 1)$, $e = 2$ and $\rho = (2)$:

$$A_{2,2}^{(2)} : \begin{array}{|c|c|c|c|c|c|c|c|} \hline 2 & 1 & 0 & 1 & 2 & 2 & 1 & 0 \\ \hline & 2 & & & & & & \\ \hline \end{array}, \quad D_{2+1}^{(2)} : \begin{array}{|c|c|c|c|c|c|c|c|} \hline 2 & 1 & 0 & 0 & 1 & 2 & 2 & 1 \\ \hline & 2 & & & & & & \\ \hline \end{array},$$

$$\begin{aligned}
 A_{2,2}^{(2)} : \mathbf{1}_\lambda^y &= \begin{array}{c} | \quad | \\ 0 \quad 0 \end{array} \quad \begin{array}{c} 0 \quad 0 \\ | \quad | \\ \vdots \quad \vdots \\ 1 \quad 1 \end{array} \quad \begin{array}{c} 1 \quad 1 \quad 1 \\ | \quad | \quad | \\ \vdots \quad \vdots \quad \vdots \\ 2 \quad 2 \quad 2 \end{array}, \\
 D_{2+1}^{(2)} : \mathbf{1}_\lambda^y &= \begin{array}{c} | \quad | \quad | \\ 1 \quad 1 \quad 1 \end{array} \quad \begin{array}{c} 1 \quad 1 \quad 1 \\ | \quad | \quad | \\ \vdots \quad \vdots \quad \vdots \\ 2 \quad 2 \quad 0 \end{array} \quad \begin{array}{c} 0 \quad 0 \\ | \quad | \\ \vdots \quad \vdots \\ 2 \quad 2 \end{array}.
 \end{aligned}$$

(c) Finally, consider $\lambda = (7, 2)$ for $e = 2$ and $\rho = (0)$. Then:

$$\begin{aligned}
 A_{2,2}^{(2)} : & \begin{array}{|c|c|c|c|c|c|c|} \hline 0 & 1 & 2 & 2 & 1 & 0 & 1 \\ \hline 1 & 0 & & & & & \\ \hline \end{array}, \quad D_{2+1}^{(2)} : \begin{array}{|c|c|c|c|c|c|c|} \hline 0 & 1 & 2 & 2 & 1 & 0 & 0 \\ \hline & 0 & 1 & & & & \\ \hline \end{array}, \\
 A_{2,2}^{(2)} : \mathbf{1}_\lambda^y &= \begin{array}{c} | \quad | \quad | \\ 0 \quad 0 \quad 0 \end{array} \quad \begin{array}{c} 0 \quad 0 \quad 0 \\ | \quad | \quad | \\ \vdots \quad \vdots \quad \vdots \\ 1 \quad 1 \quad 1 \end{array} \quad \begin{array}{c} 1 \quad 1 \quad 1 \\ | \quad | \quad | \\ \vdots \quad \vdots \quad \vdots \\ 2 \quad 2 \end{array}, \\
 D_{2+1}^{(2)} : \mathbf{1}_\lambda^y &= \begin{array}{c} | \quad | \quad | \\ 1 \quad 1 \quad 1 \end{array} \quad \begin{array}{c} 1 \quad 1 \quad 1 \\ | \quad | \quad | \\ \vdots \quad \vdots \quad \vdots \\ 0 \quad 0 \quad 2 \end{array} \quad \begin{array}{c} 0 \quad 0 \\ | \quad | \\ \vdots \quad \vdots \\ 0 \quad 0 \end{array}.
 \end{aligned}$$

Again, note the different dot placements for types $A_{2,2}^{(2)}$ and $D_{2+1}^{(2)}$.

All of these pictures were created using TikZ macros defined in the preamble. \diamond

Example 5E.7. We continue with Example 5D.6. Recall that $n = 3$, $e = 2$, $\ell = 1$ and $\kappa = (0)$, and fix $\rho = (0)$, so $\underline{\ell} = 10$. Let $\lambda_1 = (3|\emptyset|\dots|\emptyset)$, $\lambda_2 = (2, 1|\emptyset|\dots|\emptyset)$ and $\lambda_3 = (1^3|\emptyset|\dots|\emptyset)$, and also $\mu_1 = (2|1|\emptyset|\dots|\emptyset)$ and $\mu_2 = (1|1|1|\emptyset|\dots|\emptyset)$. These five diagrams have the following dotted idempotent diagrams for type $A_{2,2}^{(2)}$:

$$\begin{aligned}
 \mathbf{1}_{\lambda_1}^y &= \begin{array}{c} | \quad | \\ 0 \quad 0 \end{array} \quad \begin{array}{c} 0 \\ | \\ \vdots \\ 1 \end{array} \quad \begin{array}{c} 1 \\ | \\ \vdots \\ 2 \end{array}, \quad \mathbf{1}_{\lambda_2}^y = \begin{array}{c} | \quad | \\ 0 \quad 0 \end{array} \quad \begin{array}{c} 0 \\ | \\ \vdots \\ 1 \end{array} \quad \begin{array}{c} 1 \\ | \\ \vdots \\ 2 \end{array} \quad \begin{array}{c} 1 \\ | \\ \vdots \\ 1 \end{array}, \\
 \mathbf{1}_{\lambda_3}^y &= \begin{array}{c} | \quad | \\ 0 \quad 0 \end{array} \quad \begin{array}{c} 0 \\ | \\ \vdots \\ 1 \end{array} \quad \begin{array}{c} 1 \\ | \\ \vdots \\ 2 \end{array}, \\
 \mathbf{1}_{\mu_1}^y &= \begin{array}{c} | \quad | \\ 0 \quad 0 \end{array} \quad \begin{array}{c} 0 \\ | \\ \vdots \\ 1 \end{array} \quad \begin{array}{c} 1 \\ | \\ \vdots \\ 0 \end{array} \quad \begin{array}{c} 0 \\ | \\ \vdots \\ 0 \end{array}, \\
 \mathbf{1}_{\mu_2}^y &= \begin{array}{c} | \quad | \\ 0 \quad 0 \end{array} \quad \begin{array}{c} 0 \\ | \\ \vdots \\ 0 \end{array} \quad \begin{array}{c} 0 \\ | \\ \vdots \\ 0 \end{array} \quad \begin{array}{c} 0 \\ | \\ \vdots \\ 0 \end{array}.
 \end{aligned}$$

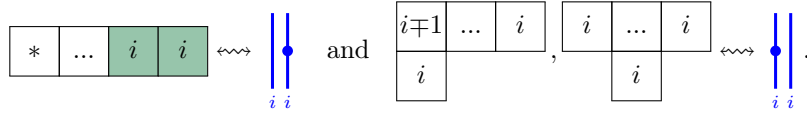
Here, we have drawn affine red strings only for the final two diagrams. The dotted idempotents for type $D_{e+1}^{(2)}$ look similar, but since there is no ghost 0-string the 1 and 2 strings move to the left. For example

$$\mathbf{1}_{\lambda_1}^y = \begin{array}{c} | \\ 1 \end{array} \quad \begin{array}{c} 1 \\ | \quad | \\ \vdots \quad \vdots \\ 2 \quad 0 \end{array}$$

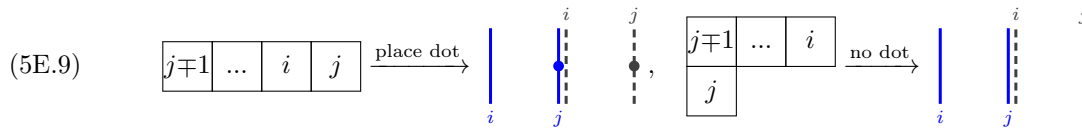
is the diagram for $\mathbf{1}_{\lambda_1}^y$ for type $D_{2+1}^{(2)}$. \diamond

Lemma 5E.8. *We have $\mathbf{1}_\lambda^y = \mathbf{1}_\mu^y$ if and only if $\lambda = \mu$.*

Proof. One direction is immediate, so let us assume that $\lambda \neq \mu$. If $\text{res}_\rho(\lambda) \neq \text{res}_\rho(\mu)$, then $\mathbf{1}_\lambda^y \neq \mathbf{1}_\mu^y$ follows using the faithful polynomial module from Remark 3D.2. Moreover, a different dot placement on the same idempotent diagram $\mathbf{1}_\lambda$ can also be distinguished by Remark 3D.2, so it remains to show that $\mathbf{1}_\lambda^y$ and $\mathbf{1}_\mu^y$ have different dot placements if $\text{res}_\rho(\lambda) = \text{res}_\rho(\mu)$. To see this assume that the k th node, in row reading order, is the first node that is different for λ and μ . By the minimality of k , we can assume that the k th node of μ is in a new row when compared to the k th node of λ . There are three cases to check now, depending on the residue j of the k th string and the residue i of the $(k-1)$ th string. When $i = j$ is a multisink the local diagrams for λ and μ are:



As required, these diagrams have different dot placements. The case $i \rightsquigarrow j$ for shifted partitions is illustrated in (5E.4), while



is the case for usual partitions. The case $i \leftarrow j$ is similar to (5E.4) and (5E.9). Hence, in all cases the dot placements in $\mathbf{1}_\lambda^y$ and $\mathbf{1}_\mu^y$ are different, so the lemma is proved. \square

5F. The sandwiched part. The following configuration of close strings is needed in Definition 5F.2:



(This diagram does not arise if i has no ghost.) In this diagram we have highlighted the j -string, which can get a dot in the sandwiched part.

Definition 5F.2. Define the set of *affine dots* as

$$A^y(\lambda) = \{ \mathbf{a} = (a_1, \dots, a_n) \in \mathbb{Z}_{\geq 0}^n \mid a_k = 0 \text{ whenever } \mathbf{x}_{\kappa}(\lambda)_k \leq \max_{\mathbb{R}}(\text{fin}) \}.$$

For $1 \leq k \leq n$, define $c_k(\lambda) = 1$ if the k th string is close as in (5F.1), or its partner relation, and this string does not already have a dot in $\mathbf{1}_\mu^y$ for some $\mu \in \underline{\mathbb{P}}_{\ell, n}^{\rho, \text{all}}$ with $\mathbf{1}_\lambda = \mathbf{1}_\mu$, and otherwise set $c_k(\lambda) = 0$. Define the set of *finite dots* to be

$$F^y(\lambda) = \{ \mathbf{f} = (f_1, \dots, f_n) \in \{0, 1\}^n \mid 0 \leq f_k \leq c_k(\lambda) \}.$$

The set of *sandwiched dots* is $S^y(\lambda) = A^y(\lambda) \cup F^y(\lambda)$. Note that $a_k \neq 0$ only happens for affine coordinates $\mathbf{x}_{\kappa}(\lambda)_k > \max_{\mathbb{R}}(\text{fin})$.

Example 5F.3. We continue with Example 5E.7. The condition $\mathbf{x}_{\kappa}(\lambda)_k \leq \max_{\mathbb{R}}(\text{fin})$ implies that $A^y(\lambda_1) = A^y(\lambda_2) = A^y(\lambda_3) = \{(0, 0, 0)\}$. Moreover, all strings associated to the second and third component have affine coordinates so $A^y(\mu_1) = \{(0, 0, n) \mid n \in \mathbb{Z}_{\geq 0}\}$ and $A^y(\mu_2) = \{(0, m, n) \mid m, n \in \mathbb{Z}_{\geq 0}\}$.

For the finite dots, in type $A_{2,2}^{(2)}$ we have $F^y(\lambda_1) = F^y(\lambda_3) = \{(0, 0, 0), (0, 0, 1)\}$ and $F^y(\lambda_2) = F^y(\mu_1) = F^y(\mu_2) = \{(0, 0, 0)\}$. For type $D_{3+1}^{(2)}$ the finite dots are same except that $F^y(\lambda_1) = \{(0, 0, 0), (0, 0, 1)\}$. \diamond

5G. Permutation diagrams. We need the same tableaux as in AC types. That is, let $\mathbf{x}_{\kappa}^A(-)$ be the type A positioning function, see [MT21, Definition 6A.4], which, in the notation of this paper is

$$\mathbf{x}_{\kappa}^A(m, r, c) = \kappa_m - \frac{m}{\ell} + r(k) + k\varepsilon,$$

where $k = o_\lambda(m, r, c)$ is the number given by the row reading order.

Definition 5G.1. Let $\lambda, \mu \in \underline{\mathbb{P}}_{\ell, n}^{\rho, \text{all}}$. A λ -tableau of type μ is a bijection $T: \lambda \rightarrow \mathbf{x}_{\kappa}^A(\mu)$. Such a tableau is *semistandard* if:

- (a) $T(m, 1, 1) \leq \kappa_m$ for $1 \leq m \leq \ell$.
- (b) $T(m, r, c) + 1 > T(m, r-1, c)$ for all $(m, r, c), (m, r-1, c) \in \lambda$.
- (c) $T(m, r, c) > T(m, r, c-1) + 1$ for all? $(m, r, c), (m, r, c-1) \in \lambda$.

Let $\text{SStd}_{\underline{\kappa}}(\lambda, \mu)$ be the set of semistandard λ -tableaux of type μ and set $\text{SStd}_{\underline{\kappa}}(\lambda) = \bigcup_{\mu} \text{SStd}_{\underline{\kappa}}(\lambda, \mu)$.

Definition 5G.2. For $T \in \text{SStd}_{\underline{\kappa}}(\lambda, \mu)$ define the permutation $w_T \in \mathfrak{S}_n$ by requiring that

$$x_{w_T(k)}^{\mu} = T(m, r, c) \text{ whenever } x_k^{\lambda} = x_{\underline{\kappa}}^A(m, r, c), \quad \text{for } 1 \leq k \leq n \text{ and } (m, r, c) \in \lambda.$$

This defines the *permutation diagram* $D_T = D(w_T)$ from $\mathbf{x}_{\underline{\kappa}}(\mu)$ to $\mathbf{x}_{\underline{\kappa}}(\lambda)$, as in [Notation 3C.2](#).

In other words, a semistandard λ -tableau T of type μ is a filling of the nodes of λ with the type A coordinates of μ , together with an anchor condition, such that the fillings decrease along rows and columns with an offset of 1. The associated permutation has top points defined by $\mathbf{x}_{\underline{\kappa}}(\lambda)$, bottom points by $\mathbf{x}_{\underline{\kappa}}(\mu)$ and permutes them according to the entries of T .

Example 5G.3. For $e = 2$ let $n = 6$, $\ell = 1$, $\kappa = (0)$ and $\varepsilon = 0.05$. Fix $\lambda = (5, 1)$ and $\mu = (3, 2, 1)$ for $\rho = (2)$. Then $\mathbf{x}_{\underline{\kappa}}^A(\lambda) = (-0.15, -0.05, 0.9, 1.85, 2.8, 3.75)$ and $\mathbf{x}_{\underline{\kappa}}^A(\mu) = (-0.25, -0.15, -0.05, 0.8, 0.9, 1.85)$. Two semistandard λ -tableaux, one of type λ and one of type μ , are:

$$S = \begin{array}{|c|c|c|c|c|} \hline -0.05 & 0.9 & 1.85 & 2.8 & 3.75 \\ \hline & -0.15 & & & \\ \hline \end{array}, \quad D_S = 1_{\lambda}, \quad T = \begin{array}{|c|c|c|c|c|} \hline -0.15 & 0.8 & -0.05 & 0.9 & 1.85 \\ \hline & -0.25 & & & \\ \hline \end{array} \rightsquigarrow \begin{array}{c} \begin{array}{|c|c|c|c|} \hline | & | & | & | \\ \hline \end{array} \\ \text{X} \\ \begin{array}{|c|c|c|c|} \hline | & | & | & | \\ \hline \end{array} \end{array} \begin{array}{c} \mathbf{x}_{\underline{\kappa}}^A(\lambda) \\ \uparrow \text{read} \\ \mathbf{x}_{\underline{\kappa}}^A(\mu) \end{array}.$$

The tableau S is the *canonical λ -tableau* of type λ , where all nodes are filled with their coordinates. Its associated permutation diagram is the identity. The permutation diagram D_T is build from the permutation illustrated above, which connects $\mathbf{x}_{\underline{\kappa}}^A(\mu)$ to $\mathbf{x}_{\underline{\kappa}}^A(\lambda)$, using $\mathbf{x}_{\underline{\kappa}}(\mu)$ at the bottom and $\mathbf{x}_{\underline{\kappa}}(\lambda)$ at the top. \diamond

Example 5G.4. Related to our main example from [Example 4A.2](#). We use the numbers from [Example 5D.7](#), e.g. $\frac{m}{\ell} = \frac{1}{19}$ and $\varepsilon = 0.001$. In this case, the type A positioning function gives

$$\begin{array}{|c|c|c|c|} \hline -0.052 & 0.949 & 1.950 & 1.951 \\ \hline & -0.048 & 0.953 & \\ \hline \end{array}.$$

In particular, going from this multitableau to itself, we can only permute the two solid 2-strings without violating the condition of being standard. This gives precisely the four possible permutation diagrams from [Example 4A.2](#). \diamond

5H. Basis diagrams. Before we can define our cellular bases we first need to fix a set X of endpoints for our diagrams.

An *addable node* of λ is a node $(m, r, c) \notin \lambda$ such that $\lambda \cup \{(m, r, c)\}$ is the diagram of a ρ -partition.

Definition 5H.1. Let $\underline{P}_{\ell,0}^{\rho} = \{(\emptyset | \dots | \emptyset)\}$. For $n \geq 1$, let $\underline{P}_{\ell,n}^{\rho}$ be the subset of $\underline{P}_{\ell,n}^{\rho,all}$ defined by the condition that $\lambda \in \underline{P}_{\ell,n}^{\rho}$ only if $\lambda = \mu \cup \alpha$, where $\mu \in \underline{P}_{\ell,n-1}^{\rho}$ and α is an addable i -node of μ such that:

$$\text{whenever } \beta \text{ is an addable } i\text{-node of } \mu \text{ with } \mathbf{x}_{\underline{\kappa}}(\beta) < \mathbf{x}_{\underline{\kappa}}(\alpha), \text{ then } \mathbf{x}_{\underline{\kappa}}(\beta) \leq \max_{\mathbb{R}}(\text{fin}).$$

Finally, let $X = \bigcup_{\lambda} \mathbf{x}_{\underline{\kappa}}(\lambda)$ be the set of all coordinates, for $\lambda \in \underline{P}_{\ell,n}^{\rho}$.

Remark 5H.2. In general, only a handful of the elements of $\underline{P}_{\ell,n}^{\rho,all}$ belong to $\underline{P}_{\ell,n}^{\rho}$ as the rule in [Definition 5H.1](#) only allows the addition of affine nodes that are not too far to the right.

We are ready for our main definition:

Definition 5H.3. For $\lambda \in \underline{P}_{\ell,n}^{\rho}$ set $\mathbb{S}_{\lambda}^{\mathbf{a},\mathbf{f}} = y^{\mathbf{a}} y^{\mathbf{f}} \mathbf{1}_{\lambda}^y$ and define

$$(5H.4) \quad D_{ST}^{\mathbf{a},\mathbf{f}} = (D_S)^* \mathbb{S}_{\lambda}^{\mathbf{a},\mathbf{f}} D_T$$

for $\mathbf{a} = (a_1, \dots, a_n) \in A^y(\lambda)$, $\mathbf{f} = (f_1, \dots, f_n) \in F^y(\lambda)$, $S \in \text{SStd}_{\underline{\kappa}}(\lambda, \nu)$, $T \in \text{SStd}_{\underline{\kappa}}(\lambda, \mu)$.

Remark 5H.5. Note that we use $D_{ST}^{\mathbf{a},\mathbf{f}}$ in (5H.4) to distinguish it from the abstract definition of [Definition 2A.2](#). Of course, we will show that these elements are examples of the C_{ST}^b in this definition.

We call $\mathbb{S}_{\lambda}^{\mathbf{a},\mathbf{f}} = y^{\mathbf{a}} y^{\mathbf{f}} \mathbf{1}_{\lambda}^y$ the *sandwiched part*, $y^{\mathbf{a}}$ the *affine part*, and $y^{\mathbf{f}}$ the *finite part* of $D_{ST}^{\mathbf{a},\mathbf{f}}$. The following are the bases that we consider.

Definition 5H.6. Let $\mathbb{S}_{\lambda}^{\mathbf{f}} = \mathbb{S}_{\lambda}^{(0,\dots,0),\mathbf{f}}$ and $D_{ST}^{\mathbf{f}} = D_{ST}^{(0,\dots,0),\mathbf{f}}$. We define

$$(5H.7) \quad D_{\mathcal{W}_n^{\rho}(X)}^{\mathbf{a},\mathbf{f}} = \{D_{ST}^{\mathbf{a},\mathbf{f}} \mid \lambda \in \underline{P}_{\ell,n}^{\rho}, S, T \in \text{SStd}_{\underline{\kappa}}(\lambda), \mathbf{a} \in A^y(\lambda), \mathbf{f} \in F^y(\lambda)\}.$$

$$(5H.8) \quad D_{\mathcal{O}_n^{\rho}(X)}^{\mathbf{f}} = \{D_{ST}^{\mathbf{f}} \mid \lambda \in \underline{P}_{\ell,n}^{\rho}, S, T \in \text{SStd}_{\underline{\kappa}}(\lambda), \mathbf{f} \in F^y(\lambda)\}.$$

5I. Homogeneous (affine) sandwich cellular bases. The sandwich cellular partial order, which we define below, is the same as in [MT21, Definition 7C.1]. In essence, we measure how far solid strings are to the right, with diagrams becoming bigger in the partial order as we move solid strings to the right.

Definition 5I.1. Let $\lambda, \mu \in \underline{P}_{\ell, n}^{\rho}$. Then λ *dominates* μ , written $\lambda \trianglerighteq \mu$, if there exists a bijection $d: \lambda \rightarrow \mu$ such that $\mathbf{x}_{\kappa}(\alpha) \geq \mathbf{x}_{\kappa}(d(\alpha))$ and the solid string in $\mathbf{1}_{\lambda}$ at position $\mathbf{x}_{\kappa}(\alpha)$ has at least as many dots as the solid string in $\mathbf{1}_{\mu}$ at position $\mathbf{x}_{\kappa}(d(\alpha))$, for all $\alpha \in \lambda$. Write $\lambda \triangleright \mu$ if $\lambda \trianglerighteq \mu$ and $\lambda \neq \mu$.

We are now ready to define (involutive) bases for $\mathscr{W}_n^{\rho}(X)$ and $\mathscr{R}_n^{\rho}(X)$. Recall that we are working with *BAD* types. We also use the Q -polynomials from (3A.3).

The cell datum $\mathscr{C} = (\underline{P}_{\ell, n}^{\rho}, T, \mathbb{S}, B, D, \deg, (-)^*)$ that we use is:

- The middle set is $\underline{P}_{\ell, n}^{\rho} = (\underline{P}_{\ell, n}^{\rho}, \trianglerighteq)$,
- $T = \bigcup_{\lambda \in \underline{P}_{\ell, n}^{\rho}} \text{SStd}_{\kappa}$ is the bottom/top set,
- the bases of the sandwiched algebras are $B_{\lambda} = \{\mathbb{S}_{\lambda}^{\mathbf{a}, \mathbf{f}} \mid \mathbf{a} \in A^y(\lambda), \mathbf{f} \in F^y(\lambda)\}$ for $\lambda \in \underline{P}_{\ell, n}^{\rho}$, and the sandwiched algebras \mathbb{S}_{λ} are the subalgebras of the weighted KLRW algebra generated by these bases,
- we take $D = D_{\mathscr{W}_n^{\rho}(X)}$ from (5H.7), viewed as a map, as our basis,
- the degree is $\mathbf{S} \mapsto \deg D_{\mathbf{S}}$,
- the antiinvolution is the diagrammatic antiinvolution $(-)^*$.

The proof of the following theorem is postponed until Section 6 below.

Theorem 5I.2. *The datum \mathscr{C} is a graded affine sandwich cell datum for $\mathscr{W}_n^{\rho}(X)$. In particular, (5H.7) is a homogeneous affine sandwich cellular basis for $\mathscr{W}_n^{\rho}(X)$.*

If we replace $B_{\lambda} = \{\mathbb{S}_{\lambda}^{\mathbf{a}, \mathbf{f}} \mid \mathbf{a} \in A^y(\lambda), \mathbf{f} \in F^y(\lambda)\}$ with $B_{\lambda}^c = \{\mathbb{S}_{\lambda}^{\mathbf{f}} \mid \mathbf{f} \in F^y(\lambda)\}$, and $D_{\mathscr{W}_n^{\rho}(X)}$ with $D_{\mathscr{R}_n^{\rho}(X)}$, then Theorem 5I.2 and the definitions directly imply:

Corollary 5I.3. *The datum $\mathscr{C} = (\underline{P}_{\ell, n}^{\rho}, T, \mathbb{S}^c, B^c, D_{\mathscr{R}_n^{\rho}(X)}, \deg, (-)^*)$ is a graded sandwich cell datum for $\mathscr{R}_n^{\rho}(X)$. In particular, (5H.8) is a homogeneous sandwich cellular basis for $\mathscr{R}_n^{\rho}(X)$. \square*

Define a semistandard tableaux $S \in \text{SStd}_{\kappa}(\lambda)$ to be *standard* if it is of type $\omega = (n|0|\dots|0)$. Let $\text{Std}(\lambda)$ be the set of standard λ -tableaux. Let $\mathscr{W}_n^{\rho} = \mathbf{1}_{\omega} \mathscr{W}_n^{\rho}(X) \mathbf{1}_{\omega}$ and $\mathscr{R}_n^{\rho} = \mathbf{1}_{\omega} \mathscr{R}_n^{\rho}(X) \mathbf{1}_{\omega}$ be the associated KLR and cyclotomic KLR algebra, respectively. This terminology is justified at the end of Section 3C. We use E instead of D to refer to the basis elements of the idempotent truncations. We will not highlight the cell datum below.

Proposition 5I.4. *The set $E_{\mathscr{W}_n^{\rho}(X)} = \{E_{st}^{\mathbf{a}, \mathbf{f}} \mid \lambda \in \underline{P}_{\ell, n}^{\rho}, \mathbf{S}, \mathbf{T} \in \text{Std}(\lambda), \mathbf{a} \in A^y(\lambda), \mathbf{f} \in F^y(\lambda)\}$ is a homogeneous affine sandwich cellular basis of \mathscr{W}_n^{ρ} .*

Proof. Apply [MT21, Proposition 3F.1 and Example 6A.11]. \square

As before we obtain:

Corollary 5I.5. *The set $E_{\mathscr{R}_n^{\rho}(X)} = \{E_{st}^{\mathbf{f}} \mid \lambda \in \underline{P}_{\ell, n}^{\rho}, \mathbf{S}, \mathbf{T} \in \text{Std}(\lambda), \mathbf{f} \in F^y(\lambda)\}$ is a homogeneous sandwich cellular basis of \mathscr{R}_n^{ρ} . \square*

Let us now discuss the upshot of Theorem 5I.2 and Corollary 5I.3 for simple modules. To this end, let $a(\lambda)$ and $f(\lambda)$ be the number of possible nonzero positions of $A^y(\lambda)$ and $F^y(\lambda)$, respectively.

Lemma 5I.6. *For all $\lambda \in \underline{P}_{\ell, n}^{\rho}$ we have $\mathbb{S}_{\lambda} \cong R[X_1, \dots, X_{a(\lambda)}] \otimes R[Y_1, \dots, Y_{f(\lambda)}] / (Y_1^2, \dots, Y_{f(\lambda)}^2)$ and $\mathbb{S}_{\lambda}^c \cong R[Y_1, \dots, Y_{f(\lambda)}] / (Y_1^2, \dots, Y_{f(\lambda)}^2)$.*

Proof. The first claim, regarding the X_i , follows by using Proposition 3D.1. For the second claim, regarding the Y_i , we pull strings and jump dots to the right and use Corollary 5I.3. That is, if one of the strings, which corresponds to one of the possible nonzero positions of $F^y(\lambda)$, carries two dots we can use (4A.9) and the claim follows. \square

Proposition 5I.7. *The algebra $\mathscr{R}_n^{\rho}(X)$ is free of rank $\sum_{\lambda \in \underline{P}_{\ell, n}^{\rho}} 2^{f(\lambda)} (\#\text{SStd}_{\kappa})^2$, and $\mathscr{W}_n^{\rho}(X)$ is free of rank $\sum_{\lambda \in \underline{P}_{\ell, n}^{\rho}} 2^{f(\lambda)} (\#\text{Std})^2$.*

Proof. Directly from Lemma 5I.6 and the corollaries above. \square

By the above, it is also easy to write down the graded dimensions of these algebras.

Remark 5I.8. Proposition 5I.7 generalizes the dimension formulas from [AP14, Corollary 3.5] and [AP16, Corollary 3.3].

Example 5I.9. It is illustrative to compare the combinatorics for types $C_2^{(1)}$, $A_{2,2}^{(2)}$ and $D_{2+1}^{(2)}$. (See [MT21, Section 7] for the relevant constructions in type $C_e^{(1)}$.) We will ignore the affine part in this example. Fix $\ell = 1$, $\kappa = (0)$ and $\rho = (0)$ and take $\beta = (0, 1, 2) \in I^3$. We are first looking for all 1-partitions of 3 that have β as their *residue sequence*, that is, $\lambda \in \mathbb{P}_{\ell,4}^\rho$ whose nodes have residues β in row reading order. We get the following 1-partitions:

$$C_2^{(1)}, A_{2,2}^{(2)}, D_{2+1}^{(2)}: \lambda_1 = \begin{array}{|c|c|c|} \hline 0 & 1 & 2 \\ \hline \end{array}, \quad C_2^{(1)}, A_{2,2}^{(2)}: \lambda_3 = \begin{array}{|c|} \hline 0 \\ \hline 1 \\ \hline 2 \\ \hline \end{array}.$$

The dotted idempotents for types $A_{2,2}^{(2)}$ and $D_{2+1}^{(2)}$ are displayed in Example 5E.7, and the ones for type $C_2^{(1)}$ have the same form as the ones for type $A_{2,2}^{(2)}$. The sets of finite dots for types $A_{2,2}^{(2)}$ and $D_{2+1}^{(2)}$ are listed in Example 5F.3, while the set of finite dots is always trivial in type $C_2^{(1)}$. Thus, we get by using Theorem 5I.2 that

| $\beta = (0, 1, 2)$ | $C_2^{(1)}$ | $A_{2,2}^{(2)}$ | $D_{2+1}^{(2)}$ | $\beta' = (2, 1, 0)$ | $C_2^{(1)}$ | $A_{2,2}^{(2)}$ | $D_{2+1}^{(2)}$ |
|---------------------|-------------|----------------------|-----------------|----------------------|-------------|-----------------|-----------------|
| # tableaux | 2 | 2 | 1 | # tableaux | 2 | 1 | 1 |
| graded dim | $1 + q^2$ | $(1 + q^2)(1 + q^4)$ | $1 + q^2$ | graded dim | $1 + q^2$ | 1 | $1 + q^2$ |

Here we have listed the graded dimension (using the usual q -notation indicating the degree) of the idempotent truncation of $\mathcal{R}_\beta^\rho(X)$ determined by β . We also listed the relevant numbers for $\beta' = (2, 1, 0)$ where $\rho = (2)$. These numbers match [HS21, Theorem 1.1], which is expected as this case is the cyclotomic KLR algebra of the respective types. The reader is also invited to compare the graded dimension formula from Example 4A.2 to [HS21, Theorem 1.1]; again we get the same result as expected. \diamond

Proposition 5I.10. *Suppose that R is a field, and let $(\underline{\mathbb{P}}_{\ell,n}^\rho)^{\neq 0}$ or $(\mathbb{P}_{\ell,n}^\rho)^{\neq 0}$ be the sets of apexes.*

- (a) *For a fixed apex $\lambda \in (\underline{\mathbb{P}}_{\ell,n}^\rho)^{\neq 0}$ there exist a 1:1-correspondence between simple $\mathcal{W}_n^\rho(X)$ -modules with apex λ and $R^{a(\lambda)}$. Moreover, up to isomorphism, there exists exactly one graded simple $\mathcal{W}_n^\rho(X)$ -module of that apex.*
- (b) *For a fixed apex $\lambda \in (\mathbb{P}_{\ell,n}^\rho)^{\neq 0}$ there exists exactly one simple, and one graded simple, $\mathcal{R}_n^\rho(X)$ -module of that apex up to isomorphism.*

Proof. This is a combination of Theorem 2A.4 and the results from this section. For example, the explicit parametrization of the simple modules for fixed apexes follows from Lemma 5I.6. \square

Explicitly identifying the sets $(\underline{\mathbb{P}}_{\ell,n}^\rho)^{\neq 0}$ or $(\mathbb{P}_{\ell,n}^\rho)^{\neq 0}$ of apexes is nontrivial, and we do not consider this in this paper.

6. PROOF OF CELLULARITY

We are now ready to prove Theorem 5I.2, which shows that the weighted KLRW algebras are sandwich cellular algebras.

Remark 6A.1. As before, the combinatorics below is separated into partition and shifted partition combinatorics. The former is very similar to type $C_e^{(1)}$, which was covered in [MT21, Section 7], so we focus only on the shifted partition case.

As in [MT21, Section 7E] the most important notion that we need is that of Young equivalence. To define it we need some preliminary definitions.

Definition 6A.2. For $i, j \in I$, a *close (i, i, i) -triple*, respectively a *close (i, j, k) -triple* or a *close (i, j, j, i) -quadruple*, is a collection of close strings as in the following local configurations:

$$(6A.3) \quad \text{triple: } \begin{array}{|c|} \hline \vdots \\ \hline iii \\ \hline \end{array}, \quad \text{triple: } \left(\begin{array}{|c|} \hline \begin{array}{c} i k \\ \vdots \\ j \end{array} \\ \hline \end{array} \text{ or } \begin{array}{|c|} \hline \begin{array}{c} j \\ \vdots \\ i k \end{array} \\ \hline \end{array} \right) \quad \text{and} \quad \left(\text{quadruple: } \begin{array}{|c|} \hline \begin{array}{c} i i \\ \vdots \\ j j \end{array} \\ \hline \end{array} \text{ or } \begin{array}{|c|} \hline \begin{array}{c} j j \\ \vdots \\ i i \end{array} \\ \hline \end{array} \right).$$

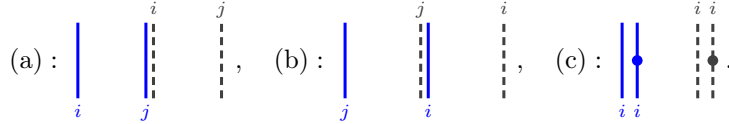
We also need the following, which should be compared with Remark 5D.10. Here we consider the two ghost 1-strings in type $D_{e+1}^{(2)}$ as one string.

Definition 6A.4. Let S be a dotted straight line diagram. Solid i and j -strings of S are *pseudo row equivalent* if either:

- (a) $i \rightsquigarrow j$, there are no dots on the i or j -strings, and the ghost i -string is close and to the left of the solid j -string;
- (b) $i \leftarrow j$, there are no dots on the i or j -strings, and the solid i -string is close and to the left of the ghost j -string;
- (c) $i = j$ is a multisink, the i -string carries a dot, and the solid i -string is close and to the right of the solid j -string;

A **row equivalence class** is a pseudo row equivalence class in which there are no close (i, i, i) -triples, the only close (i, j, k) -triples are of the form $(i, i + 1, i + 2)$ or $(i, i - 1, i - 2)$, or $(1, 0, 1)$ in type $A_{2e}^{(2)}$, and if (i, j, j, i) is a close quadruple, then j is a multisink and either $i \rightsquigarrow j$ or $i \leftarrow j$.

The illustrations for parts (a)–(c) of [Definition 6A.4](#) are:



These should be compared with [\(5D.11\)](#) and [\(5D.13\)](#). Note that [\(5D.12\)](#) is also included in the description since pseudo row equivalence classes only consider two solid strings at a time.

By definition, there is a unique **first** and **last** string in each row equivalence class because the strings in a row equivalence class are ordered by closeness, starting with the string that is not close and to the right of any other in the same class.

Definition 6A.5. Assume that we are in the case of shifted partitions. A **Young equivalence class** Y is a disjoint union of row equivalence classes $R_1 \cup \dots \cup R_z$ such that:

- (a) The first string in R_1 has no dot and is close to an (affine) red string of the same residue;
- (b) $|R_1| > |R_2| > \dots > |R_z|$;
- (c) The first string in R_{a+1} is an i -string that is close to a dotted solid i -string of the same residue in R_a , or there is a j -string in R_a that satisfies one of closeness conditions in (a) and (b) of [Definition 6A.4](#), with respect to this string.

For partitions, we use the analog of [\[MT21, Definition 7E.6\]](#). That is, part (b) is replaced with $|R_1| \geq |R_2| \geq \dots \geq |R_z|$ and (c) mimics [\(5D.14\)](#) with a dot on the i -string in the first two cases therein.

Recall that $L(S)$ is the left-justification of the dotted straight line diagram S as e.g. in [Example 3C.5](#).

Lemma 6A.6. Let S be a dotted straight line diagram. Then $L(S) = L(\mathbf{1}_\lambda^y)$, for some $\lambda \in \underline{\mathcal{P}}_{\ell, n}^p$, if and only if the solid strings of S are a disjoint union of Young equivalence classes.

Proof. By construction, the solid strings in $\mathbf{1}_\lambda^y$ are a disjoint union of Young equivalence classes cf. [Remark 5D.10](#).

To prove the converse, given a dotted straight line diagram S , we construct an ℓ -partition λ by inductively associating the solid strings in each Young equivalence class Y to nodes in a component $\lambda^{(m)}$ of λ . We explain the situation of shifted partitions, which is when ρ_m is a multisink. The case of partitions can be proven similarly, following [\[MT21, Lemma 7E.8\]](#).

By [Definition 6A.5\(a\)](#), the first string of Y is left adjacent to an (affine) red string of the same residue. If this is the m th red string, then identify the solid string with the node $(m, 1, 1)$. By induction we now assume that the k th solid i -string in Y corresponds to the node $(m, r, c) \in \lambda$ and consider the $(k + 1)$ st solid j -string. There are two cases to consider.

Case 1. First, if i is not the last string in its row equivalence class, then [\(5D.11\)](#), [\(5D.12\)](#) and [\(5D.13\)](#) correspond to (a)–(c) of [Definition 6A.4](#) and the condition on close (i, j, k) -triples and close (j, i, i, j) -quadruples, with the correct dot placement. Moreover, no other configurations can appear, i.e. there are no close (i, i, i) -triples or any other triples or quadruples due to (a)–(c) of [Definition 6A.4](#). Hence, the $(k + 1)$ st solid j -string corresponds to the node $(m, r, c + 1)$.

Case 2. If on the other hand i is the last string in its row equivalence class, then we observe that [\(5D.14\)](#) corresponds to [Definition 6A.5\(c\)](#), and the $(k + 1)$ st solid j -string corresponds to the node $(m, r + 1, c)$.

Finally, note that the condition in [Definition 6A.5\(b\)](#) ensures that the resulting diagram is a shifted ℓ -partition. \square

Proposition 6A.7. Suppose that $D \in \mathcal{W}_n^\rho(X)$ and that D factors through the dotted idempotent diagram S . Then there exists $\lambda \in \underline{\mathcal{P}}_{\ell, n}^p$ such that D factors through $\mathbf{1}_\lambda^y$ and $\lambda \succeq L(S)$.

Proof. Without loss of generality we can assume that $D = S$. If $D = \mathbf{1}_\lambda^y$, then there is nothing to prove by Lemma 6A.6. So assume that Lemma 6A.6 is not satisfied, so that D is not a disjoint union of Young equivalence classes.

We can assume that all strings are within $[\min X, \max X + 1] \times [0, 1]$, the *region defined by X* . Let s be the rightmost solid string in D that is not in any Young equivalence class. We want to argue that we can pull s to the right, jump dots on s further to the right, or we can attach s to a Young equivalence class, which implies the claim by induction. There are a few cases which we need to discuss. We only consider shifted partition combinatorics since the arguments for usual partition combinatorics are mutatis mutandis as in [MT21, Proposition 7E.9].

Case 1a. s is the rightmost string in the sense that we can pull it arbitrarily far to the right, and s does not have a dot. In this case we can park it next to an affine red string of the same residue, and it is now part of a Young equivalence class by Definition 6A.5.(a).

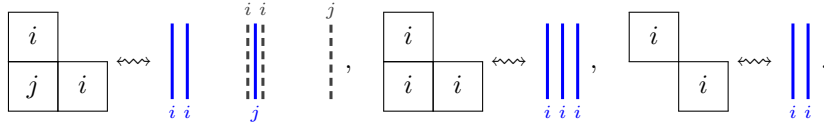
Case 1b. As in Case 1a, but now s carries a dot. After pulling the dot to the top of the diagram we are back in Case 1a.

We now assume that we are not in Cases 1a and 1b. Then, up to isotopy, s or its ghost is close and to the right of a solid, ghost or red string t . We focus on the situation when s is close to t , where we again have several cases. The cases where the ghost of s is close to t follow mutatis mutandis and are omitted. We also assume that s does not carry a dot. If it does, then there is an additional extra argument one needs, as is explained in [MT21, Proof of Proposition 7E.9, Case 5] (this argument works mutatis mutandis in the BAD types), but in the end the relation used below allow us to continue with the induction.

Case 2a. Assume that s is not in the Young equivalence class of t because s does not satisfy the close (i, j, k) -triple condition because s is the leftmost string in (6A.3). In this case the right-hand relation in (4A.8) applies, so we can pull s further to the right. (This works unless we in a close $(1, 0, 1)$ -triple situation in type $A_{2,e}^{(2)}$, in which case s and t are in the same Young equivalence class by Definition 6A.4.)

Case 2b. Similarly, assume that s is not in the Young equivalence class of t because s does not satisfy the close (i, j, j, i) -quadruple condition because s is the leftmost string in (6A.3). Then we can use Lemma 4A.10 to pull s further to the right.

Case 2c. We now assume that s is not in the Young equivalence class of t because the condition $|R_1| > |R_2| > \dots > |R_z|$ is not satisfied. For $i, j \in I$ and $i \rightsquigarrow j$ or $i \leftarrow j$, the crucial configurations are



There are a few cases, but for all these we can use (4A.7) or (4A.8) to pull s to the right.

Assume now that we are not in any of the cases above.

Case 3a. If t is an (affine) red string, then an honest Reidemeister II relation pulls s further to the right. We can apply such a relation since the case where s has the same residue as t is, which case s is the first string in a row equivalence class.

Case 3b. If t is a solid string, then an honest Reidemeister II relation applies unless s has the same residue as t . In this latter case (4A.7) applies.

Case 3c. Finally, if t is a ghost string, then we can use an honest Reidemeister II relation to pull s to the right. An honest Reidemeister II relation applies because the assumption that s and t are not in the same Young equivalence class implies that s and t do not satisfy the conditions of (a) and (b) of Definition 6A.4, or Definition 6A.5.(c).

Hence, the result follows by induction. \square

The rest of the proof of Theorem 5I.2 is essentially the same as in [MT21, Section 7E]. That is, applying dots or crossings to $\mathbf{1}_\lambda^y$ gives a linear combination of bigger elements. To this end, recall the definition of the finite dots and the integers $c_m(\lambda)$ from Definition 5F.2.

Lemma 6A.8. *Suppose that $\lambda \in \underline{P}_{\ell,n}^p$ and $1 \leq m \leq n$. Then $y_m y_m^{c_m(\lambda)} \mathbf{1}_\lambda^y \in \mathscr{W}_n^{\triangleright \lambda}$.*

Proof. By Proposition 6A.7, the diagram $y_m y_m^{c_m(\lambda)} \mathbf{1}_\lambda^y$ factors through $\mathbf{1}_\mu^y$, for some $\mu \triangleright \lambda$. \square

By ignoring the components, consider λ as a composition, and let \mathfrak{S}_λ be the associated Young subgroup of \mathfrak{S}_n .

Lemma 6A.9. *Suppose that $\lambda \in \underline{P}_{\ell,n}^p$ and $w \in \mathfrak{S}_\lambda$. Then $D_\lambda(w) \mathbf{1}_\lambda, \mathbf{1}_\lambda D_\lambda(w) \in \mathscr{W}_n^{\triangleright \lambda}$.*

Proof. As in [MT21, Lemma 6D.17]. \square

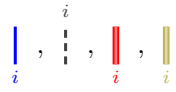
Proof of Theorem 5I.2. The arguments given in [MT21, Sections 6D and 7E], which are the analogous statements for the AC types, apply in BAD types as well. In fact, these arguments are general and use only Proposition 3D.1 and Remark 3D.2, as well as the analogs of the results proven above. \square

Remark 6A.10. Following the strategy in Remark 4A.1, the construction of the homogeneous (affine) sandwich cellular basis and proof of Theorem 5I.2 splits into several parts:

- (a) Because the bottom and top of the cellular basis elements are given by permutation diagrams, the first step is to find suitable tableau combinatorics for the quiver under study. For a general quiver this is potentially hopeless, and one might want to use some other combinatorial data instead of tableaux, but for a lot of quivers an answer is already in the literature.
- (b) The construction of the middle in Remark 2A.3 is then crucial. This part is noncanonical, although mostly dictated by Remark 4A.1. We hope to explain a more general approach in future work. Note that additional dots might be necessary to prevent basis elements being annihilated by (3A.6) and to ensure that we have the analog of Lemma 5E.8.
- (c) From here onwards the arguments are general and do not depend on the quiver anymore: Proposition 6A.7 follows by analyzing the combinatorics of the string placement of $\mathbf{1}_\lambda$, and this proposition in turn directly implies Lemma 6A.8 and Lemma 6A.9. Once these two lemmas have been established the proof of cellularity Theorem 5I.2 is formal. Linear independence follows using the faithful polynomial module in Remark 3D.2, spanning using Lemma 6A.8 and Lemma 6A.9 and the standard basis in Proposition 3D.1. The latter arguments are independent of the underlying quiver.

7. TABLE OF NOTATION AND CENTRAL CONCEPTS

In general we use an overline for notation that only plays a role in the infinite dimensional setting.

| Name | Symbol | Description |
|--|--|---|
| Solid, ghost, red and affine strings |  | Strings in diagrams, see (3A.1) |
| ℓ =level, κ =charge | $n, \ell, e, \kappa, \rho, X$ | The number of solid strings, the number of red strings, the number of vertices in the quiver, the positions of the red strings, the labels of the red strings, the positions and labels of the solid strings; all of these are fixed from the start, see Section 3A |
| Affine notation | $\underline{\ell}, \underline{\kappa}, \underline{\rho}$ | We set $\underline{\ell} = \ell + n(e + 1)$. These ensure that we have enough affine red string to catch every solid string, see Section 5B |
| Weighted KLRW algebra | $\mathscr{W}_n^\rho(X)$ | A diagram algebra with n solid strings with top and bottom x -coordinates in X , see Section 3A |
| The cyclotomic version | $\mathscr{R}_n^\rho(X)$ | A quotient of $\mathscr{W}_n^\rho(X)$, cf. (3A.11) |
| Idempotent diagram for λ | $\mathbf{1}_\lambda$ | The idempotent diagram created by inductively placing strings while reading along the rows of the $\underline{\rho}$ -partition λ , see Section 5D |
| The dotted version of $\mathbf{1}_\lambda$ | $\mathbf{1}_\lambda^y$ | We place dots y_λ on $\mathbf{1}_\lambda$, see Section 5E |
| Affine and finite part | y^a and y^f | These determine the sandwiched part of the main basis; the affine part only plays a role for $\mathscr{W}_n^\rho(X)$, while the finite part appears for both $\mathscr{W}_n^\rho(X)$ and $\mathscr{R}_n^\rho(X)$, see Section 5F |
| Permutation diagram for \mathcal{S} | $D_{\mathcal{S}}$ | A permutation diagram associated to the $\underline{\rho}$ -tableaux \mathcal{S} , see Section 5G |
| Sandwiched algebras | \mathbb{S}_λ | The sandwiched algebras are tensor products of $R[X]$ and $R[X]/(X^2)$, see Section 5I |
| Cellular basis elements | $D_{\mathcal{ST}}^{a,f}, D_{\mathcal{ST}}^f$ | The homogeneous cellular basis elements, see Section 5I, for $\mathscr{W}_n^\rho(X)$ and $\mathscr{R}_n^\rho(X)$ |
| Cellular basis sets | $D_{\mathscr{W}_n^\rho(X)}, D_{\mathscr{R}_n^\rho(X)}$ | The homogeneous cellular bases sets, see Section 5I, for $\mathscr{W}_n^\rho(X)$ and $\mathscr{R}_n^\rho(X)$ |

| Name | Symbol | Description |
|--|--|--|
| Cellular bases for the KLR(W) algebras | $\mathcal{W}_n^\rho, \mathcal{R}_n^\rho, E_{\mathcal{W}_n^\rho(X)}, E_{\mathcal{R}_n^\rho(X)}$ | The KLR(W) algebras $\mathcal{W}_n^\rho, \mathcal{R}_n^\rho$ arise via idempotent truncation and $E_{\mathcal{W}_n^\rho(X)}, E_{\mathcal{R}_n^\rho(X)}$ are the corresponding homogeneous cellular bases |
| Partitions | $\underline{P}_{\ell,n}^\rho, P_{\ell,n}^\rho$ | Indexing sets for the middle of the cellular bases of $\mathcal{W}_n^\rho(X)$ and $\mathcal{R}_n^\rho(X)$, see Section 5C |
| Nodes | (m, r, c) | Nodes in (shifted) partitions: m is the component index, r the row index and c the column index, see Remark 5C.3 |
| Simple modules | $(\underline{P}_{\ell,n}^\rho)^{\neq 0}, (P_{\ell,n}^\rho)^{\neq 0}$ | Indexing sets for the simple modules of $\mathcal{W}_n^\rho(X)$ and $\mathcal{R}_n^\rho(X)$, see Section 5I |
| Tableaux | $\text{SStd}_{\kappa}, \text{Std}$ | Indexing sets for the bottom/top of the cellular bases of $\mathcal{W}_n^\rho(X)$ and \mathcal{W}_n^ρ , cf. Section 5H |
| Positioning function | \mathbf{x}_{κ} | The function that assigns x -coordinates to nodes of Young diagrams, see Section 5D |
| Maximal finite part | $\max_{\mathbb{R}}(\text{fin})$ | Determines where the affine part of the diagrams begin, see Section 5D |

REFERENCES

- [AP14] S. Ariki and E. Park. Representation type of finite quiver Hecke algebras of type $A_{2\ell}^{(2)}$. *J. Algebra*, 397:457–488, 2014. URL: <https://arxiv.org/abs/1208.0889>, doi:10.1016/j.jalgebra.2013.09.005.
- [AP16] S. Ariki and E. Park. Representation type of finite quiver Hecke algebras of type $D_{\ell+1}^{(2)}$. *Trans. Amer. Math. Soc.*, 368(5):3211–3242, 2016. URL: <https://arxiv.org/abs/1305.6367>, doi:10.1090/tran/6411.
- [AST18] H.H. Andersen, C. Stroppel, and D. Tubbenhauer. Cellular structures using U_q -tilting modules. *Pacific J. Math.*, 292(1):21–59, 2018. URL: <https://arxiv.org/abs/1503.00224>, doi:10.2140/pjm.2018.292.21.
- [Bow22] C. Bowman. The many integral graded cellular bases of Hecke algebras of complex reflection groups. *Amer. J. Math.*, 144(2):437–504, 2022. URL: <https://arxiv.org/abs/1702.06579>, doi:10.1353/ajm.2022.0008.
- [DJM98] R. Dipper, G. James, and A. Mathas. Cyclotomic q -Schur algebras. *Math. Z.*, 229(3):385–416, 1998. doi:10.1007/PL00004665.
- [ET21] M. Ehrig and D. Tubbenhauer. Relative cellular algebras. *Transform. Groups*, 26(1):229–277, 2021. URL: <https://arxiv.org/abs/1710.02851>, doi:10.1007/S00031-019-09544-5.
- [GL96] J.J. Graham and G. Lehrer. Cellular algebras. *Invent. Math.*, 123(1):1–34, 1996. doi:10.1007/BF01232365.
- [GMS09] O. Ganyushkin, V. Mazorchuk, and B. Steinberg. On the irreducible representations of a finite semigroup. *Proc. Amer. Math. Soc.*, 137(11):3585–3592, 2009. URL: <https://arxiv.org/abs/0712.2076>, doi:10.1090/S0002-9939-09-09857-8.
- [Gre51] J.A. Green. On the structure of semigroups. *Ann. of Math. (2)*, 54:163–172, 1951. doi:10.2307/1969317.
- [GW15] N. Guay and S. Wilcox. Almost cellular algebras. *J. Pure Appl. Algebra*, 219(9):4105–4116, 2015. doi:10.1016/j.jpaa.2015.02.010.
- [HM10] J. Hu and A. Mathas. Graded cellular bases for the cyclotomic Khovanov–Lauda–Rouquier algebras of type A . *Adv. Math.*, 225(2):598–642, 2010. URL: <http://arxiv.org/abs/0907.2985>, doi:10.1016/j.aim.2010.03.002.
- [HS21] J. Hu and L. Shi. Graded dimensions and monomial bases for the cyclotomic quiver Hecke algebras. 2021. URL: <https://arxiv.org/abs/2108.05508>.
- [Kac90] V.G. Kac. *Infinite-dimensional Lie algebras*. Cambridge University Press, Cambridge, third edition, 1990. doi:10.1017/CB09780511626234.
- [KL09] M. Khovanov and A.D. Lauda. A diagrammatic approach to categorification of quantum groups. I. *Represent. Theory*, 13:309–347, 2009. URL: <https://arxiv.org/abs/0803.4121>, doi:10.1090/S1088-4165-09-00346-X.
- [KL11] M. Khovanov and A.D. Lauda. A diagrammatic approach to categorification of quantum groups II. *Trans. Amer. Math. Soc.*, 363(5):2685–2700, 2011. URL: <https://arxiv.org/abs/0804.2080>, doi:10.1090/S0002-9947-2010-05210-9.
- [KL15] A.S. Kleshchev and J.W. Loubert. Affine cellularity of Khovanov–Lauda–Rouquier algebras of finite types. *Int. Math. Res. Not. IMRN*, (14):5659–5709, 2015. URL: <https://arxiv.org/abs/1310.4467>, doi:10.1093/imrn/rnu096.
- [KX12] S. König and C. Xi. Affine cellular algebras. *Adv. Math.*, 229(1):139–182, 2012. doi:10.1016/j.aim.2011.08.010.
- [MT21] A. Mathas and D. Tubbenhauer. Subdivision and cellularity for weighted KLRW algebras. 2021. URL: <https://arxiv.org/abs/2111.12949>.
- [Rou08] R. Rouquier. 2-Kac–Moody algebras. 2008. URL: <http://arxiv.org/abs/0812.5023>.
- [Rou12] R. Rouquier. Quiver Hecke algebras and 2-Lie algebras. *Algebra Colloq.*, 19(2):359–410, 2012. URL: <https://arxiv.org/abs/1112.3619>, doi:10.1142/S1005386712000247.
- [Tub22] D. Tubbenhauer. Sandwich cellularity and a version of cell theory. 2022. URL: <https://arxiv.org/abs/2206.06678>.
- [TV21] D. Tubbenhauer and P. Vaz. Handlebody diagram algebras. 2021. To appear in *Rev. Mat. Iberoam*. URL: <https://arxiv.org/abs/2105.07049>, doi:10.4171/RMI/1356.
- [Web17] B. Webster. Rouquier’s conjecture and diagrammatic algebra. *Forum Math. Sigma*, 5:e27, 71, 2017. URL: <https://arxiv.org/abs/1306.0074>, doi:10.1017/fms.2017.17.
- [Web19] B. Webster. Weighted Khovanov–Lauda–Rouquier algebras. *Doc. Math.*, 24:209–250, 2019. URL: <https://arxiv.org/abs/1209.2463>, doi:10.25537/dm.2019v24.209-250.

A.M.: THE UNIVERSITY OF SYDNEY, SCHOOL OF MATHEMATICS AND STATISTICS F07, OFFICE CARSLAW 718, NSW 2006, AUSTRALIA, [WWW.MATHS.USYD.EDU.AU/U/MATHAS/](http://www.maths.usyd.edu.au/u/mathas/)
Email address: andrew.mathas@sydney.edu.au

D.T.: THE UNIVERSITY OF SYDNEY, SCHOOL OF MATHEMATICS AND STATISTICS F07, OFFICE CARSLAW 827, NSW 2006, AUSTRALIA, [WWW.DTUBBENHAUER.COM](http://www.dtubbenhauer.com)
Email address: daniel.tubbenhauer@sydney.edu.au